JOURNAL OF PETROLOGY | VOLUME 43 | NUMBER 9 | PAGES 1725–1747 | 2002

Crustal Evolution in the SW Part of the Baltic Shield: the Hf Isotope Evidence

T. ANDERSEN[1]*, W. L. GRIFFIN[2,3] AND N. J. PEARSON[2]

[1]LABORATORY OF ISOTOPE GEOLOGY, MINERALOGICAL–GEOLOGICAL MUSEUM, UNIVERSITY OF OSLO, SARS GATE 1, N-0562 OSLO, NORWAY

[2]GEMOC KEY CENTRE, DEPARTMENT OF EARTH AND PLANETARY SCIENCES, MACQUARIE UNIVERSITY, SYDNEY, N.S.W. 2109, AUSTRALIA

[3]CSIRO EXPLORATION AND MINING, NORTH RYDE, N.S.W. 2113, AUSTRALIA

RECEIVED MAY 23, 2001; REVISED TYPESCRIPT ACCEPTED MARCH 12, 2002

The results of a laser ablation microprobe–inductively coupled plasma mass spectrometry Lu–Hf isotope study of zircons in 0·93–1·67 Ga rocks from south Norway indicate that early Proterozoic protoliths of the Baltic Shield have present-day $^{176}Hf/^{177}Hf \leq 0{\cdot}28190$ [$\varepsilon_{Hf}(t) = 5$–6], *whereas 1·52–1·60 Ga juvenile additions to the continental margin have* $^{176}Hf/^{177}Hf = 0{\cdot}2820$ [$\varepsilon_{Hf}(t) = 12$–13]. *Mid- to late Proterozoic felsic igneous rocks in the region are characterized by a range of Hf isotopic compositions suggesting mixing of material derived from Palaeoproterozoic crust from the Baltic Shield and/or mid-Proterozoic juvenile crust. New mantle-derived magmas were added to the crust at ∼1·48 Ga and in Sveconorwegian time. Late Sveconorwegian granites from the area west of the Oslo Rift have inherited zircons with low* $^{176}Hf/^{177}Hf$ ($<0{\cdot}28180$), *suggesting that a pre-1·7 Ga crustal source contributed to the magmas. The evolution of the continental crust in this region is thus a result of repeated interaction between mantle-derived magmas and mid- to early Proterozoic crustal rocks. The results of this study confirm the presence of early Proterozoic rocks in the deep crust west of the Oslo Rift, and support tectonic models in which the protolith of the western part of south Norway has been part of the Baltic Shield since the early Proterozoic.*

KEY WORDS: *hafnium isotopes; Baltic Shield; continental crust; crustal evolution*

INTRODUCTION

The lutetium–hafnium radiogenic isotope system gives information that more or less duplicates that provided by the more widely used samarium–neodymium system (e.g. Dickin, 1995). As a tracer of petrogenetic processes, however, Lu–Hf has one important advantage over Sm–Nd: zircons retain a robust memory of their initial Hf isotopic compositions, because of their high Hf concentrations, low Lu/Hf ratios and general ability to survive metamorphic processes. Zircon has the additional advantage of being datable by U–Pb techniques. A number of benchmark papers have established the hafnium isotope signatures of the most significant reservoirs in the upper mantle and continental crust, and their evolution through geological time (e.g. Patchett *et al.*, 1981; Vervoort & Patchett, 1996; Blichert-Toft & Albarède, 1997; Vervoort & Blichert-Toft, 1999; Vervoort *et al.*, 1999; Griffin *et al.*, 2000). Until recently, the need for elaborate laboratory techniques has prevented the widespread use of hafnium isotopes in zircons as a tracer of crustal evolution. However, advances in analytical technology, which include the development of stable laser ablation microprobes and multicollector, plasma-source, magnetic sector mass spectrometers, have made the *in situ* microanalysis of hafnium isotopes in zircons a matter of routine.

In this paper, we use hafnium isotope data from single zircons to gain insights into the evolution of the Precambrian crust of south Norway, which makes up the youngest and least well-understood part of the Baltic Shield. These data allow us to identify the Lu–Hf signatures of different crustal domains in the region, to trace the lateral extent of early Proterozoic crust toward the west, to examine the contributions of crustal and juvenile mantle sources to mid- and late-Proterozoic

*Corresponding author. Present address: Department of Geology, University of Oslo, PO Box 1047, Blindern, N-0316 Oslo, Norway. E-mail: tom.andersen@geologi.uio.no

igneous rocks, and to test current models for the evolution of the western margin of the Baltic Shield.

GEOLOGICAL SETTING

Regional overview

The Precambrian continental crust of Norway south of the Caledonian thrust front (Fig. 1) is part of the Southwest Scandinavian Domain (SSD) of the Baltic Shield (e.g. Gaàl & Gorbatschev, 1987). In the central and SW parts of the Baltic Shield, orogenic events have been identified in the periods 1·9–1·75 Ga (Svecofennian), 1·75–1·55 Ga ('Gothian'), and 1·2–0·9 Ga (Sveconorwegian, i.e. Grenvillian; Gaàl & Gorbatschev, 1987; Gorbatschev & Bogdanova, 1993). A large, roughly north–south-trending belt of granitic intrusions and rhyolitic porphyries (the Trans-Scandinavian Igneous Belt; TIB) was emplaced in the period 1·83–1·65 Ga (Gorbatschev & Bogdanova, 1993), and separates the Svecofennian province of Sweden in the east from 'Gothian' and Sveconorwegian terranes in SW Scandinavia (Fig. 1, inset).

Two contrasting tectonic models for the Southwest Scandinavian Domain of the Baltic Shield have been discussed in recent literature. In one of these, based on a concept originally suggested by Berthelsen (1980), present-day south Norway west of the Oslo Rift forms an exotic microcontinent, accreted onto the Baltic Shield *sensu stricto* in a collision event between 1·58 and 1·50 Ga along a suture now masked by the Palaeozoic rocks of the Oslo Rift (Åhäll *et al.*, 1998, 2000; Åhäll & Larson, 2000). Critics of this model have emphasized the similarity in geochronological and geochemical signatures across the Oslo Rift and other potential suture zones in the region, which suggest that south Norway has been an integral part of the Baltic Shield since formation of the regional protoliths at 1·7–1·9 Ga (Knudsen *et al.*, 1997*a*, 1997*b*; de Haas *et al.*, 1999; Andersen & Knudsen, 2000; Andersen *et al.*, 2001*a*; Bingen *et al.*, 2001). The recognition of subduction-related igneous rocks formed in the interval 1·6–1·52 Ga on both sides of the Oslo Rift is definite evidence that these areas all formed part of a single, destructive continental margin in the mid-Proterozoic (Andersen *et al.*, 2001*c*). These workers have therefore preferred variations on a tectonic model originally suggested by Torske (1985), in which parts of south Norway have been displaced southwards along the margin of the Baltic Shield during the Sveconorwegian orogeny (Starmer, 1996; de Haas *et al.*, 1999; Bingen *et al.*, 2001; Andersen *et al.*, 2001c).

The Precambrian of south Norway

The Precambrian crust of south Norway is divided into several domains, separated by major Sveconorwegian shear zones, some of which have been reactivated as brittle faults in Phanerozoic time. Here, the regional terminology for the SSD of Andersen & Knudsen (2000) and Lindström *et al.* (2000) is used. This is a geographical and non-genetic nomenclature; it does not assign tectonostratigraphic terrane status to any of the units, which are referred to as 'sectors' (Andersen & Knudsen, 2000) or 'segments' (Lindström *et al.*, 2001). Whether or not some or all of these represent terranes in a tectonic sense is still unclear. South Norway is transected by the late Palaeozoic Oslo Rift, which complicates reconstructions of the Precambrian crust of the area (e.g. Berthelsen, 1980; Åhäll *et al.*, 1998; de Haas *et al.*, 1999; Bingen *et al.*, 2001).

The area east of the Oslo Rift (the Østfold–Akershus Sector; ØA in Fig. 1) is a northward continuation of the Western and parts of the Eastern gneiss segments of SW Sweden (Lindström *et al.*, 2000), and consists of three major gneiss complexes (from south to north: the Østfold, Romerike and Solør complexes; Fig. 1), which are separated by Sveconorwegian shear zones (Hageskov, 1980). The Østfold complex consists of metasupracrustal gneisses, associated with several generations of granitic to tonalitic orthogneisses, interpreted as deformed intrusions. Amphibolites, meta-rhyolites and metasedimentary gneisses in the Østfold complex can be correlated with the Stora Le–Marstrand supracrustals in SW Sweden (Graversen, 1984). The Romerike complex consists of mid-Proterozoic migmatitic gneisses of possible supracrustal origin, intruded by calc-alkaline granitoids (Berthelsen *et al.*, 1996; Andersen *et al.*, 2001*c*), and the Solør complex of $\sim$1·67 Ga and older TIB-equivalent potassic granites and associated supracrustal gneisses (Hjelle, 1963; Nordgulen, 1999). The $\sim$1·67 Ga Odal granite is the southwesternmost representative of the TIB.

The Kongsberg Sector (K in Fig. 1) is characterized by supracrustal rocks and granodioritic to tonalitic gneisses (the Kongsberg complex; KC in Fig. 1), metasediments (the Modum complex; MC in Fig. 1) and granitic gneisses of uncertain origin (the Randsfjord complex), listed in sequence from SW to NE (Jacobsen, 1975; Dons & Jorde, 1978; Jacobsen & Heier, 1978; Nordgulen, 1999; Fig. 1). Detrital zircon ages from metasediments suggest that supracrustal rocks in the Modum and Kongsberg complexes can be correlated with their equivalents in the Bamble Sector and the Østfold complex, respectively (Nordgulen, 1999; Bingen *et al.*, 2001). The western boundary of the Kongsberg Sector is defined by a Sveconorwegian shear zone (the Kongsberg–Telemark boundary or KTB in Fig. 1).

The central and northern parts of the Telemark Sector (T in Fig. 1) are made up of well-preserved volcanic rocks and clastic metasediments, metamorphosed in the greenschist to lower amphibolite facies (the Telemark

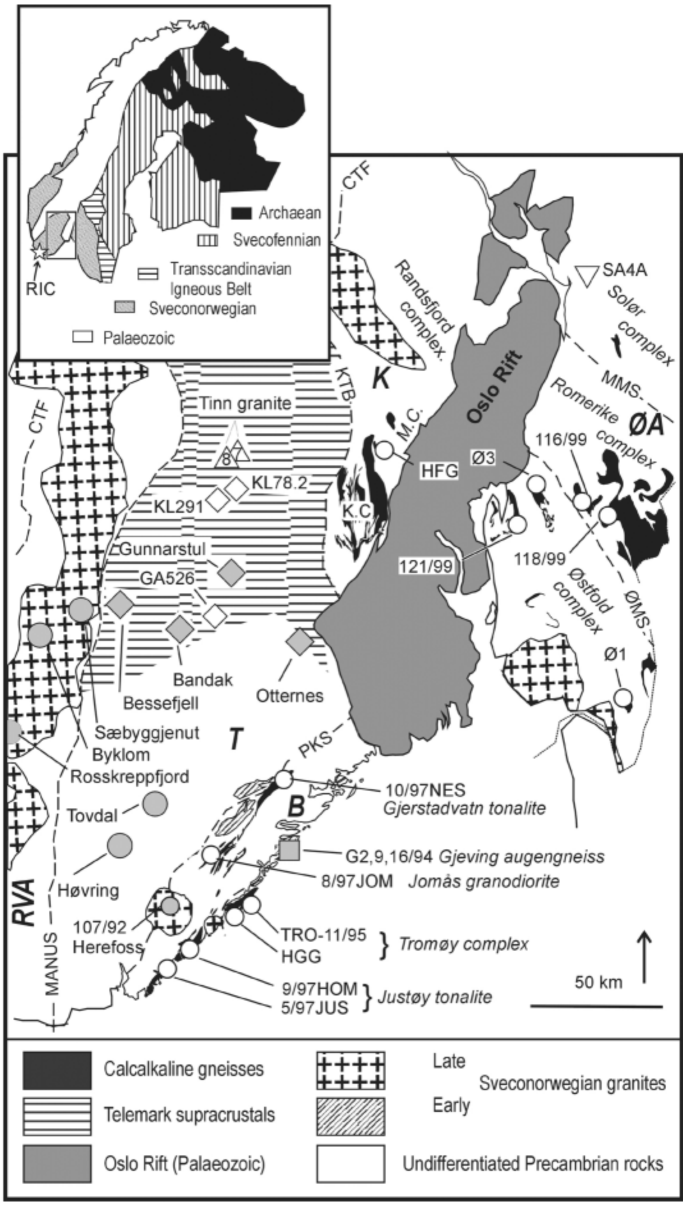

Fig. 1. Simplified geological map of south Norway, with sampling localities. ØA, Østfold–Akershus Sector; K, Kongsberg Sector; T, Telemark Sector; B, Bamble Sector; RVA, Rogaland–Vest Agder Sector. Major Precambrian (Sveconorwegian) shear zones are shown as dashed lines (MANUS, Mandal–Ustaoset line; PKS, Kristiansand–Porsgrunn shear zone; KTB, Kongsberg–Telemark boundary; ØMS, Ørje Mylonite zone; MMS, Mjøsa–Magnor shear zone). CTF, Caledonian thrust front. Samples: ○, calc-alkaline gneisses; ▽, Odal granite; △, Tinn granite (8, 083196-2; 7, 071996-2); ◇, Telemark quartzites; grey square, Sveconorwegian augengneiss; grey circles, Late Sveconorwegian 'normal Sr' granite; grey diamonds, Late Sveconorwegian 'low Sr' granite. Inset shows overview map of the Baltic Shield. RIC, 0·93 Ga Rogaland igneous complex.

supracrustals; Dons, 1960; Sigmond *et al.*, 1997). Two supracrustal sequences with distinct ages ($\sim$1·5 Ga and $\sim$1·15 Ga, respectively) are recognized in this area. The older supracrustals crop out in the northern part of the area, and comprise the 1·51–1·50 Ga meta-rhyolites and metabasalts of the Rjukan group (Dahlgren *et al.*, 1990*a*; Sigmond, 1998), with unconformably overlying quartzitic metasediments (Dons, 1960). The rhyolites of the Rjukan group were deposited in extensional basins interpreted as a continental rift by Sigmond (1997) and Sigmond *et al.* (1997). The younger supracrustal sequence crops out in the southern and southwestern part of the area, and includes quartzites (some of which have been erroneously correlated with those of the older sequence; Laajoki *et al.*, 2000), and the mixed volcanic and sedimentary sequences of the Bandak and Heddal groups. Volcanic rocks of the younger Telemark sequence have recently been dated to ~1·15 Ga (Dahlgren *et al.*, 1990*a*; Laajoki *et al.*, 2000, in preparation). South of the supracrustal area, the Telemark Sector consists of granitic gneisses of uncertain origin (e.g. Ploquin, 1972; Kleppe, 1980) and late Sveconorwegian granitic intrusions (e.g. Sylvester, 1998; Andersen *et al.*, 2001*a*).

The Bamble Sector (B in Fig. 1) consists of metasedimentary gneisses and quartzites, associated with quartzofeldspathic orthogneisses and metagabbroic rocks (Starmer, 1985; Padget & Brekke, 1996; Knudsen, 1997; Andersen *et al.*, 2001*c*). Metamorphism in the upper amphibolite to granulite facies (Nijland, 1993; Knudsen, 1996) has been dated to ~1100 Ma (Kullerud & Machado, 1991; Kullerud & Dahlgren, 1993). The Bamble Sector is separated from the Telemark Sector by a major Sveconorwegian shear zone (the Porsgrunn–Kristiansand shear zone; PKS). The Tromøy complex is a Sveconorwegian island-arc fragment, characterized by granulite-facies low-K mafic to tonalitic gneisses and anatectic trondhjemite (Knudsen & Andersen, 1999; Andersen *et al.*, 2001*c*). The age of the igneous protoliths is ~1·20 Ga, whereas high-grade metamorphism and anatexis took place at 1·13 Ga (Knudsen & Andersen, 1999).

The Rogaland–Vest Agder Sector (RVA in Fig. 1), is made up mainly of granitic gneisses with minor amounts of metasedimentary rocks (Falkum, 1982; Bingen *et al.*, 1993; de Haas *et al.*, 1999), and is separated from the Telemark Sector to the east by the Mandal–Ustaoset shear zone (MANUS line), which is probably older than ~1120 Ma, but which was reactivated during the Sveconorwegian orogeny (Sigmond, 1998). The 930 Ma anorogenic Rogaland igneous complex (Michot, 1960; Schärer *et al.*, 1996; Schiellerup *et al.*, 2000), comprising voluminous anorthosites and associated mafic intrusive rocks, makes up the southwesternmost part of the Rogaland–Vest Agder Sector (Fig. 1, inset).

Several generations of mid- to late Proterozoic granitoids are recognized in south Norway, including ~1·67 Ga TIB equivalents in the Solør complex (Nordgulen, 1999), mid-Proterozoic calc-alkaline intrusions (1·60–1·50 Ga; Nordgulen *et al.*, 1997; Andersen *et al.*, 2001*a*, 2001*c*), 1·48 Ga granites in the Telemark Sector (Andersen *et al.*, 2001*b*), three groups of deformed Sveconorwegian granites (Bingen & van Breemen, 1998), and undeformed, late Sveconorwegian 'post-tectonic' granites (Killeen & Heier, 1975; Andersen *et al.*, 2001*a*). Both mid-Proterozoic calc-alkaline granitoids and late Sveconorwegian granites are widely distributed in the region (Fig. 1), and are thus important indicators of crustal evolution. The mid-Proterozoic calc-alkaline granitoids are abundant in the Østfold–Akershus, Bamble and parts of the Kongsberg sectors, but do not occur in the Telemark and Rogaland–Vest Agder sectors (Dons & Jorde, 1978; Falkum, 1982; Berthelsen *et al.*, 1996; Padget & Brekke, 1996; Sigmond, 1998; Nordgulen, 1999).

A considerable set of Hf isotope data from the Archaean and Svecofennian domains of the Baltic Shield has been published by Patchett *et al.* (1981) and Vervoort & Patchett (1996); however, no data from TIB granitoids or from the Southwest Scandinavian Domain have been published.

Hf ISOTOPE SYSTEMATICS

The material studied

The zircons analysed in the present study were separated from (meta)igneous rocks ranging in age from 0·93 to 1·67 Ga, i.e. covering the whole age range of preserved rocks in the Precambrian of south Norway (Table 1). In addition, two well-dated detrital zircon fractions from Telemark quartzites have been included, one of which (1·8 ± 0·1 Ga, from the ~1·15 Ga Vallar Bru formation; de Haas *et al.*, 1999) represents a source of clastic material of importance in the region, older than any rocks exposed at the present-day surface (Knudsen, 1997). The other, from the ~1·5 Ga Heddersvatn formation, contains zircons of an age close to the depositional age, which must have been derived from source rocks belonging to the Rjukan group (Andersen & Laajoki, in preparation). A summary of the main characteristics of the rocks sampled is given in Table 1, and further details on individual samples are shown in Appendix 1.

Zircons have moderately elongated euhedral prismatic habits, with terminal pyramid faces. The central parts of the grains show regular oscillatory 'magmatic' zoning; infrequent xenocrystic cores show oscillatory zoning crosscut by the enclosing grain. In many cases, zircons were mounted too deep in the epoxy disc to expose small, xenocrystic cores (this was done on purpose to prevent 'blowout' of grains during ablation and to ensure maximum ablation time). In such cases, the presence of isotopically distinct cores could be identified from shifts in the time-resolved isotopic ratio profiles. Both visible cores and zircons identified as inherited from their isotopic compositions are moderately abundant in the late Sveconorwegian granites, but are rare in any of the other groups of samples studied. The 1·48 Ga Tinn granite and some of the Mesoproterozoic calc-alkaline granitoids contain a few cored zircons, whose cores are only slightly (10–20 Ma) older than the enclosing zircon and the host rock (Andersen *et al.*, 2001*c*). Most zircon grains from pre-Sveconorwegian rocks have thin back-scattered electron (BSE)-bright overgrowths, which are generally too thin for analysis (<10 μm). These are assumed to have formed in response to Sveconorwegian metamorphism.

Table 1: Summary of the main rock types sampled

Period (Ga)	Rock type	Sector	Age (Ga)	Comment	References
1·65–1·85	Quartzite	T	1·8 ± 0·1	Detrital zircons in ~1·15 Ga (younger) Telemark quartzite (Vallar Bru fm), dated by SIMS U–Pb	de Haas *et al.* (1999), Laajoki *et al.* (2000)
	Granite	ØA	1·67	The Odal granite: southwesternmost part of the Trans-Scandinavian Igneous Belt	Nordgulen (1999)
1·54–1·65	Calc-alkaline granitoids	ØA, K, B	1·53–1·60	Tonalitic and granodioritic metaintrusive gneiss complexes	Andersen *et al.* (2001*c*)
1·40–1·54	Quartzite	T	1·50	Detrital zircons in ~1·5 Ga (older) Telemark quartzite (Heddersvatn fm); zircons were dated to ~1·50 Ga by LAM–ICPMS U–Pb, and are probably derived from local rocks of the Rjukan group	Laajoki *et al.* (2000), Andersen & Laajoki (in preparation)
	Granite	T	1·48	The Tinn granite: foliated granite intruding Rjukan group meta-rhyolite	Andersen *et al.* (2001*b*)
1·15–1·40	Calc-alkaline granitoids	B	1·20	Tromøy complex metatonalite, with 1·13 Ga anatectic trondhjemite	Knudsen & Andersen (1999)
	Granite	B	1·15	Gjeving granitic augengneiss, member of the Gjerstad suite of anorogenic intrusions	Kullerud & Machado (1991), Bingen & van Breemen (1998)
	Rhyolite	T	1·15	Lavas of the younger Telemark supracrustal sequence Hf + REE cuts from dissolved zircons dated by TIMS U–Pb	Laajoki *et al.* (2000)
1·15–0·90	Granite	B, T, RVA	1·13–0·93	Late- and postorogenic granites	Andersen *et al.* (2001*a*)

For details on individual samples, see the Appendix. B, Bamble Sector; K, Kongsberg Sector; T, Telemark Sector; RVA, Rogaland–Vest Agder Sector; ØA, Østfold–Akershus Sector.

Analytical methods

Samples (5–10 kg) collected from fresh outcrops (roadcuts, building sites) were crushed to a grain size <250 μm, using a steel jaw crusher and a percussion mill. Zircons were separated by a combination of Wilfley-table washing, heavy liquid separation (1,1,2,2-tetrabromoethane and diiodomethane), magnetic separation and hand-picking. Selected zircon grains from the least magnetic fractions were cast in epoxy discs for laser ablation microprobe–multi-collector inductively coupled plasma mass spectrometry (LAM–MC-ICPMS) analysis.

Nd and Sm were separated from finely crushed and homogenized whole-rock powders by standard ion exchange procedures. The isotopic composition of Nd was determined by mass spectrometry, using a fully automated Finnigan MAT 262 mass spectrometer in the Laboratory of Isotope Geology, Mineralogical–Geological Museum, Oslo. Nd isotopic compositions are normalized to $^{146}Nd/^{144}Nd = 0{\cdot}7219$. During the period when the present analyses were made, the Johnson and Matthey batch No. S819093A Nd_2O_3 gave $^{143}Nd/^{144}Nd = 0{\cdot}511101 \pm 0{\cdot}000013$ (2σ). Concentrations of Lu, Hf, Sm and Nd were determined by fusion ICP-MS by Actlab, Canada. Additional Nd and Sm concentrations were determined by isotope dilution, using aliquots spiked in ^{150}Nd and ^{149}Sm and the MAT262 instrument as above. The ID and ICPMS concentrations agree within experimental error.

The Hf-isotope analyses reported here were carried out *in situ* using a New Wave Research LUV213 laser-ablation microprobe, attached to a Nu Plasma multi-collector ICPMS system, at Macquarie University. The laser system delivers a beam of 213 nm UV light from a frequency-quintupled Nd:YAG laser. Most analyses were carried out with a beam diameter of ∼40 μm, a 10 Hz repetition rate, and energies of 0·6–1·3 mJ/pulse. This resulted in total Hf signals of $(1–6) \times 10^{-11}$ A, depending on conditions and the Hf contents. Typical ablation times were 30–120 s, resulting in pits 20–60 μm deep. Ar carrier gas transported the ablated sample from the laser-ablation cell via a mixing chamber to the ICPMS torch.

The Nu Plasma MC-ICPMS system features a unique geometry with a fixed detector array of 12 Faraday cups and three ion counters; beams are directed into the collectors by varying the dispersion of the instrument using an electrostatic zoom lens. For this work we analysed masses 172, 175, 176, 177, 178, 179 and 180 simultaneously in Faraday cups; all analyses were carried out in static-collection mode. Data were normalized to $^{179}Hf/^{177}Hf = 0{\cdot}7325$, using an exponential correction for mass bias. Initial setup of the instrument was performed using a 1 ppm solution of JMC475 Hf, spiked with 80 ppb Yb, which typically yielded a total Hf beam of $(10–14) \times 10^{-11}$ A. The laser-ablation analyses were carried out using the Nu Plasma time-resolved analysis software, in which the signal for each mass and each ratio is displayed as a function of time during the analysis. This allows the more stable portions of the ablation to be selected for analysis, before the data are processed to give the final results. The selected interval is divided into 40 replicates for the calculation of the standard error. Background was collected on peak for 45 s before ablation began.

The measurement of accurate $^{176}Hf/^{177}Hf$ ratios in zircon requires correction of the isobaric interferences of ^{176}Lu and ^{176}Yb on ^{176}Hf. This correction is relatively straightforward for the Nu Plasma, because the mass bias of the instrument is independent of mass over the mass range considered here (Griffin *et al.*, 2000). Interference of ^{176}Lu on ^{176}Hf was corrected by measuring the intensity of the interference-free ^{175}Lu isotope and using $^{176}Lu/^{175}Lu = 0{\cdot}02669$ to calculate the intensity of ^{176}Lu. Similarly, the interference of ^{176}Yb on ^{176}Hf was corrected by measuring the interference-free ^{172}Yb isotope and using $^{176}Yb/^{172}Yb$ to calculate the intensity of ^{176}Yb. The appropriate value of $^{176}Yb/^{172}Yb$ (0·5865) was determined by successively spiking the JMC475 Hf standard (100 ppb solution) with Yb (to 40 ppb), and determining the value of $^{176}Yb/^{172}Yb$ required to yield the value of $^{176}Hf/^{177}Hf$ obtained on the pure Hf solution.

The reproducibility of Hf isotope analyses in solution has been demonstrated by repeated analysis of the JMC475 Hf standard (Table 2); our mean value for $^{176}Hf/^{177}Hf$ is $0{\cdot}282161 \pm 21$ ($n = 208$). Analysis of this solution spiked with different levels of Yb shows that good precision and accuracy are obtained on the $^{176}Hf/^{177}Hf$ ratio, despite the severe corrections on ^{176}Hf; these estimates include the propagation of error involved in the overlap correction. The JMC475 Hf (100 ppb) + Yb (40 ppb) gave an average $^{176}Hf/^{177}Hf$ of $0{\cdot}282159 \pm 60$ and demonstrates the robustness of the Yb overlap correction up to $^{176}Yb/^{177}Hf$ of ∼0·26. All zircons analysed in this study have much lower $^{176}Yb/^{177}Hf$.

The accuracy of the Yb and Lu corrections during LAM–MC-ICPMS analysis of zircon has been demonstrated by Griffin *et al.* (2000); analyses of a standard zircon 61.308, which has a wide range of $^{176}Yb/^{177}Hf$ (0·005–0·065) and $^{176}Lu/^{177}Hf$ (0·00016–0·002), showed no correlation between these ratios and $^{176}Hf/^{177}Hf$ (Table 2). The accuracy and precision of the laser-ablation analyses of $^{176}Hf/^{177}Hf$ in zircon also have been demonstrated by repeated analysis of standard zircons with a range in $^{176}Yb/^{177}Hf$ and $^{176}Lu/^{177}Hf$ (Griffin *et al.*, 2000). For most zircons >100 μm long, the typical within-run precision (2SE) on the analysis of $^{176}Hf/^{177}Hf$ is $\pm 0{\cdot}00003$, equivalent to an analytical uncertainty of one epsilon unit; on smaller zircons, with shorter run times, larger uncertainties are measured (Table 2).

Table 2: Data on Hf isotope standards

Sample	No. of analyses	Yb (ppm)	Lu (ppm)	Hf (ppm)	$^{176}Lu/^{177}Hf$	$^{176}Yb/^{177}Hf$	$^{176}Hf/^{177}Hf$	±2SD	Hf signal (V)
JMC475 Hf	208			0·1–1·0			0·282161	0·000021	5–18*
JMC475 Hf (+Yb)	27	0·04		0·105		0·260	0·282159	0·000060	0·8–4·0
	18	0·01		0·1		0·070	0·282161	0·000040	3·0–4·5
Zircon 91500	60	62·5	13·9		0·00030		0·282297	0·000044	
			12·4†						
TIMS	7		12	5895	0·00029		0·282290	0·000014	
Zircon 61308									
	45				0·00169	0·04996	0·282999	0·000083	
	12				0·00022	0·00654	0·282966	0·000113	
	22	352	78		0·00138	0·04080	0·282992	0·000093	
TIMS	9		83	5658	0·00207	n.a.	0·282975	0·000050	

Yb and Lu concentrations of zircons by LAM–ICPMS; TIMS data from Wiedenbeck *et al.* (1995). n.a., not analysed.
*Hf signal was 5–10 V for 0·1 ppm solution using MCN6000; 9–18 V for 1 ppm solution using Meinhard nebulizer.
†Lu calculated from $^{176}Lu/^{177}Hf$ and given Hf content.

The measured $^{176}Lu/^{177}Hf$ ratios are used here to calculate initial $^{176}Hf/^{177}Hf$ ratios. Griffin *et al.* (2000) showed that LAM–ICPMS analyses of $^{176}Lu/^{177}Hf$ for standard zircon 91500 gave $^{176}Lu/^{177}Hf$ within error (1σ) of the isotope dilution values. Standard zircon 61.308, as noted above, shows a wide range of Lu/Hf, and the isotope dilution value lies within this range. This indicates that Lu and Hf exhibit similar ablation characteristics, and that the $^{176}Lu/^{177}Hf$ ratios measured by LAM–MC-ICPMS are not obviously biased. The typical 2SE uncertainty on a single analysis of $^{176}Lu/^{177}Hf$ is $\pm 10\%$ or less; at the Lu/Hf ratios considered here (Table 3), this contributes an uncertainty of $<0{\cdot}1$ ε_{Hf} unit.

For the calculation of ε_{Hf} values, we have adopted the chondritic values of Blichert-Toft & Albarède (1997). These values were reported relative to $^{176}Hf/^{177}Hf = 0{\cdot}282163$ for the JMC475 standard, well within error of our reported value (Table 2). To calculate model ages based on a depleted-mantle source, we have adopted a model with $(^{176}Hf/^{177}Hf)_i = 0{\cdot}279718$ and $^{176}Lu/^{177}Hf = 0{\cdot}0384$. This produces a value of $^{176}Hf/^{177}Hf$ (0·28325) similar to that of average mid-ocean ridge basalt (MORB) over 4·56 Ga; in the time-interval of interest for this study, this mantle evolution curve is indistinguishable from the $f_{Lu/Hf} = 0{\cdot}16$ curve of Vervoort & Blichert-Toft (1999).

Mixed Lu–Hf solutions were separated by ion exchange from small zircon populations of younger Telemark rhyolites dated by thermal ionization mass spectrometry U–Pb by Laajoki *et al.* (2000, in preparation). These Hf separates were analysed on the Nu Plasma MC-ICPMS system at Macquarie University. Samples were taken up in 1 ml HNO_3 and aspirated through a CETAC MCN6000 desolvating nebulizer. The data are reported relative to our value of 0·282160 for the JMC457 Hf standard.

Calculation of sample averages, zircon and whole-rock model ages were carried out using Microsoft Excel spreadsheets written by the authors.

RESULTS

Lu–Hf isotope data for a total of 571 single zircons are plotted by chronological or petrological group in Fig. 2, which also includes published data from the Svecofennian Domain (Patchett et al., 1981; Vervoort & Patchett, 1996). The analytical data are listed in a supplementary table to this paper, available for downloading from the *Journal of Petrology* Web site at http://www.petrology.oupjournals.org or by request to the first author. Average $^{176}Hf/^{177}Hf$, $^{176}Lu/^{177}Hf$ and $^{176}Yb/^{177}Lu$ of individual samples are given in Table 3, together with data for 'outliers', which are statistically valid analyses whose time-corrected $^{176}Hf/^{177}Hf$ deviates significantly from the average ratio of the main zircon population of their host rock. These zircons must have been derived from sources other than those that contributed the hafnium contained in the bulk of the zircons in the rock, and may represent inherited material. However, the range of $^{176}Hf/^{177}Hf$ recorded in the main zircon populations of most samples is well outside analytical uncertainties. This probably reflects the generation of the sampled magma by the accumulation and mixing of magmas derived from several different source rocks; some of the 'outliers' may reflect the isotopic composition of individual magma batches that contributed to the final magma that crystallized the bulk of the analysed zircons. Such magma mixing has been documented in detailed studies of single magmatic complexes (Griffin *et al.*, 2002). In some cases it is reflected in Hf-isotope zoning within single zircon grains, whereas in others it shows up as a range of Hf-isotope compositions that may be correlated with different zircon populations.

As is common for zircons, $^{176}Lu/^{177}Hf$ ratios are low ($<0{\cdot}006$) for all samples. The Lu–Hf whole-rock solutions give significantly lower analytical errors in the Lu/Hf ratio than the laser analyses (Fig. 2b). This is because Lu/Hf ratios commonly vary significantly on the scale of microns across single zircon grains, reflecting oscillatory zoning during magmatic crystallization (e.g. Griffin *et al.*, 2002). Because the Lu/Hf ratios of the zircons are very low, this Lu/Hf variation cannot be reflected in measurable variations in $^{176}Hf/^{177}Hf$ except perhaps in very old zircons. The precision with which the mean Lu/Hf ratio can be measured by LAM–MC-ICPMS is constrained by this internal variation, which reflects a real geological uncertainty. This geological uncertainty is lost during the solution analysis of a zircon, which yields an average value of Lu/Hf with a greater, but spurious, precision constrained only by the analytical technique. However, because Lu/Hf is so low in zircon, the dominant source of error in time-corrected $^{176}Hf/^{177}Hf$ analyses is the analytical error in the isotopic ratio, and not the error in the element ratio.

The depleted mantle model age (t_{DM}) of a mineral or rock in the continental crust reflects the time since the hafnium contained by the system was last in isotopic equilibrium with a depleted mantle reservoir; t_{DM} is therefore an estimate of the crustal residence age for the protolith. However, because of the low Lu/Hf ratio of zircon, a model age calculated from the measured $^{176}Hf/^{177}Hf$ and $^{176}Lu/^{177}Hf$ ratios of a zircon (t_{DMZ}) gives only a minimum limit for the crustal residence age of the hafnium in the zircon (Fig. 3a). If the crystallization age of the zircon is known, it is possible to calculate a more realistic model age for its host rock, the whole-rock model age (t_{DMW}), by forcing a growth curve for a system with a Lu/Hf ratio corresponding to the whole-rock through the zircon initial ratio. By combining the average

Table 3: Lu–Hf data on zircons

Sample	Complex	Age (Ga)		$^{176}Hf/^{177}Hf$	2σ	$^{176}Lu/^{177}Hf$	2σ	$^{176}Yb/^{177}Hf$	2σ	$\varepsilon_{Hf}(t)$	2σ	t_{DMZ} (Ga)	t_{DMW} (Ga)	2σ
Late Sveconorwegian granites														
107/92	Herefoss	0·93	Average	0·282147	0·000336	0·0007	0·0002	0·020	0·008	0·9	0·9	1·49	1·7	0·6
	Herefoss	0·93	Outlier	0·281720	0·000062	0·0006	0·0000	0·017	0·000	−16·3	1·1	2·06	2·4	0·1
	Herefoss	0·93	Outlier	0·281779	0·000196	0·0005	0·0000	0·012	0·001	−14·2	3·5	1·97	2·3	0·3
072396-3	Tovdal	0·94	Average	0·282230	0·000271	0·0012	0·0017	0·038	0·053	3·7	1·9	1·40	1·5	0·5
	Tovdal	0·94	Outlier	0·281933	0·000104	0·0011	0·0000	0·028	0·001	−8·9	1·8	1·80	2·1	0·2
083096-3	Byklom	0·98	Average	0·282213	0·000148	0·0008	0·0004	0·023	0·008	0·5	1·7	1·41	1·5	0·2
080296-4	Rosskreppfjord	1·04	Average	0·282230	0·000093	0·0010	0·0008	0·031	0·022	4·1	0·7	1·40	1·4	0·1
082996-2	Høvring	0·94	Average	0·282164	0·000117	0·0017	0·0016	0·055	0·055	−1·2	0·6	1·51	1·6	0·2
	Høvring	0·94	Outlier	0·281953	0·000112	0·0013	0·0001	0·050	0·004	−8·4	2·0	1·78	2·0	0·2
072496-3	Sæbyggjenut	0·94	Average	0·282211	0·000145	0·0014	0·0011	0·045	0·033	1·9	1·5	1·44	1·5	0·2
072196-3	Bandak	0·93	Average	0·282331	0·000362	0·0049	0·0036	0·167	0·152	0·5	1·6	1·40	1·5	0·6
072496-2	Bessefjell	0·93	Average	0·282216	0·000154	0·0020	0·0019	0·050	0·044	0·4	0·8	1·45	1·5	0·2
072696-2	Otternes	1·09	Average	0·282409	0·000180	0·0037	0·0023	0·137	0·095	8·4	0·8	1·24	1·4	0·6
	Otternes	1·09	Outlier	0·282646	0·000082	0·0045	0·0008	0·159	0·028	17·2	1·5	0·92	0·9	0·1
083196–1	Gunnarstul	1·13	Average	0·282266	0·000160	0·0022	0·0023	0·076	0·093	6·3	1·0	1·39	1·5	0·3
Mid-Proterozoic granite, Telemark														
071996-2	Tinn	1·48	Average	0·282087	0·000211	0·0019	0·0011	0·060	0·046	7·5	1·0	1·63	1·7	0·5
071996-2	Tinn	1·48	Outlier	0·282316	0·000132	0·0019	0·0001	0·071	0·005	16·0	2·3	1·31	1·3	0·2
083196-2	Tinn	1·48	Average	0·282106	0·000150	0·0021	0·0015	0·074	0·060	8·5	0·6	1·61	1·7	0·3
Sveconorwegian granitic augengneiss ('Gjerstad suite')														
G 9/94	Gjeving	1·15	Average	0·282102	0·000042	0·0013	0·0006	0·041	0·023	1·9	0·4	1·58	1·7	0·1
G16/94	Gjeving	1·15	Average	0·282176	0·000069	0·0012	0·0012	0·132	0·867	−0·7	0·9	1·48	1·6	0·1
G2/94	Gjeving	1·15	Average	0·282178	0·000177	0·0010	0·0011	0·033	0·037	4·8	0·4	1·47	1·6	0·3
		1·15		0·282144	0·000095	0·0012	0·0010	0·093	0·653	0·7	0·7	1·52	1·6	0·2
TIB granite														
SA4A	Odal	1·67	Average	0·281838	0·000179	0·0011	0·0006	0·034	0·096	5·2	0·4	1·93	2·0	0·3
	Odal	1·67	Outlier	0·281498	0·000220	0·0013	0·0002	0·030	0·000	−2·5	1·4	2·39	2·6	0·4
		1·67	Outlier	0·281639	0·000078	0·0007	0·0001	0·022	0·003	−8·1	3·9	2·17	2·3	0·1

Table 3: continued

Sample	Complex	Age (Ga)		$^{176}Hf/^{177}Hf$	2σ	$^{176}Lu/^{177}Hf$	2σ	$^{176}Yb/^{177}Hf$	2σ	$\varepsilon_{Hf}(t)$	2σ	t_{DMZ} (Ga)	t_{DMW} (Ga)	2σ
Sveconorwegian Tromøy arc fragment														
TRO11/95	Tromøy	1·20	Average	0·282229	0·000047	0·0012	0·0007	0·029	0·019	5·2	0·6	1·40	*1·5*	*0·1*
HGG	Hisøy	1·20	Average	0·282191	0·000108	0·0019	0·0018	0·055	0·053	7·2	0·3	1·48	1·8	*0·3*
Mid-Proterozoic calc-alkaline gneiss complexes														
HFG	Snarum	1·54	Average	0·282009	0·000076	0·0012	0·0007	0·038	0·024	7·0	0·6	1·70	*1·8*	*0·1*
HFG		1·54	Outlier	0·282106	0·000040	0·0014	0·0001	0·046	0·003	10·4	0·7	1·58	*1·6*	*0·1*
TA121/99	Sørmarka	1·54	Average	0·281998	0·000072	0·0015	0·0014	0·046	0·047	6·8	0·6	1·73	1·8	*0·1*
Ø3	Feiring	1·60	Average	0·282010	0·000109	0·0005	0·0004	0·015	0·011	9·0	1·1	1·67	1·7	*0·2*
Ø1	Tistedal	1·58	Average	0·281986	0·000094	0·0013	0·0009	0·037	0·027	6·6	0·4	1·74	1·8	*0·2*
TA116/99	Midtskog	1·58	Average	0·281992	0·000124	0·0009	0·0005	0·023	0·017	7·4	0·6	1·71	1·8	*0·2*
TA118/99	Bjørkelangen	1·58	Average	0·281968	0·000112	0·0005	0·0005	0·012	0·013	7·6	0·8	1·72	1·7	*0·2*
10/97NES	Gjerstadvatn	1·60	Average	0·282053	0·000078	0·0015	0·0006	0·046	0·020	9·3	1·0	1·66	1·7	*0·1*
8/97JOM	Jomås	1·53	Average	0·282046	0·000104	0·0006	0·0003	0·014	0·014	9·0	1·6	1·63	1·7	*0·2*
5/97JUS	Justøy–Justøy	1·59	Average	0·282112	0·000075	0·0010	0·0006	0·030	0·021	12·6	1·0	1·55	1·6	*0·1*
9/97HOM	Justøy–Homborsund	1·59	Average	0·282141	0·000099	0·0015	0·0010	0·042	0·033	12·4	0·6	1·54	1·5	*0·2*
9/97HOM	Justøy–Homborsund	1·59	Outlier	0·282267	0·000040	0·0017	0·0001	0·041	0·003	16·9	0·7	1·37	*1·3*	*0·1*
Detrital zircons, Telemark supracrustals														
KL291	Heddersvatn fm	1·50	Average	0·282051	0·000389	0·0018	0·0011	0·049	0·030	8·3	3·5	1·67	*1·7*	*0·7*
KL78·2	Heddersvatn fm	1·50	Average	0·282088	0·000123	0·0020	0·0009	0·055	0·028	7·8	0·6	1·63	*1·7*	*0·2*
KL78·2	Heddersvatn fm	1·50	Outlier	0·281923	0·000050	0·0012	0·0001	0·032	0·002	3·2	0·9	1·82	*1·9*	*0·1*
GA 526	Vallar Bru fm	1·80	Average	0·281707	0·000400	0·0011	0·0028	0·023	0·020	5·7	0·5	2·10	*2·2*	*0·7*
GA 526	Vallar Bru fm	1·80	Outlier	0·280999	0·000048	0·0004	0·0000	0·010	0·000	9·5	1·2	2·98	*3·4*	*0·1*
Young Telemark rhyolites														
903 KL-N	Brunkeberg fm	1·15	Fractions	0·282117	0·000006	0·0008	0·0001	0·026		2·6	0·2	1·54	*1·7*	*0·0*
TA 99/2 O	Heddal gr	1·15	Fractions	0·282169	0·000059	0·0010	0·0003	0·035		4·2	2·1	1·48	*1·6*	*0·1*
830 O13	Ofte fm	1·15	Fractions	0·282130	0·000017	0·0008	0·0001	0·028		3·1	0·6	1·52	1·6	*0·0*

Average, average of single zircon analyses; outlier, single-zircon analysis deviating from the sample average by more than two standard deviations, i.e. zircons whose compositions deviate significantly from the mean of the main population of the sample. The averages are given with two standard deviations; errors in single analyses are given by 2 internal standard errors for the individual analysis. t_{DMW} values in italics are based on an average whole-rock $^{176}Lu/^{177}Hf = 0{\cdot}010$, the others on estimated whole-rock $^{176}Lu/^{177}Hf$ from Table 4. The two samples from the Justøy complex give averages plotting slightly above the depleted mantle curve, and thus give t_{DMW} less than the intrusive age. $\varepsilon_{Hf}(t)$ is calculated at the ages given.

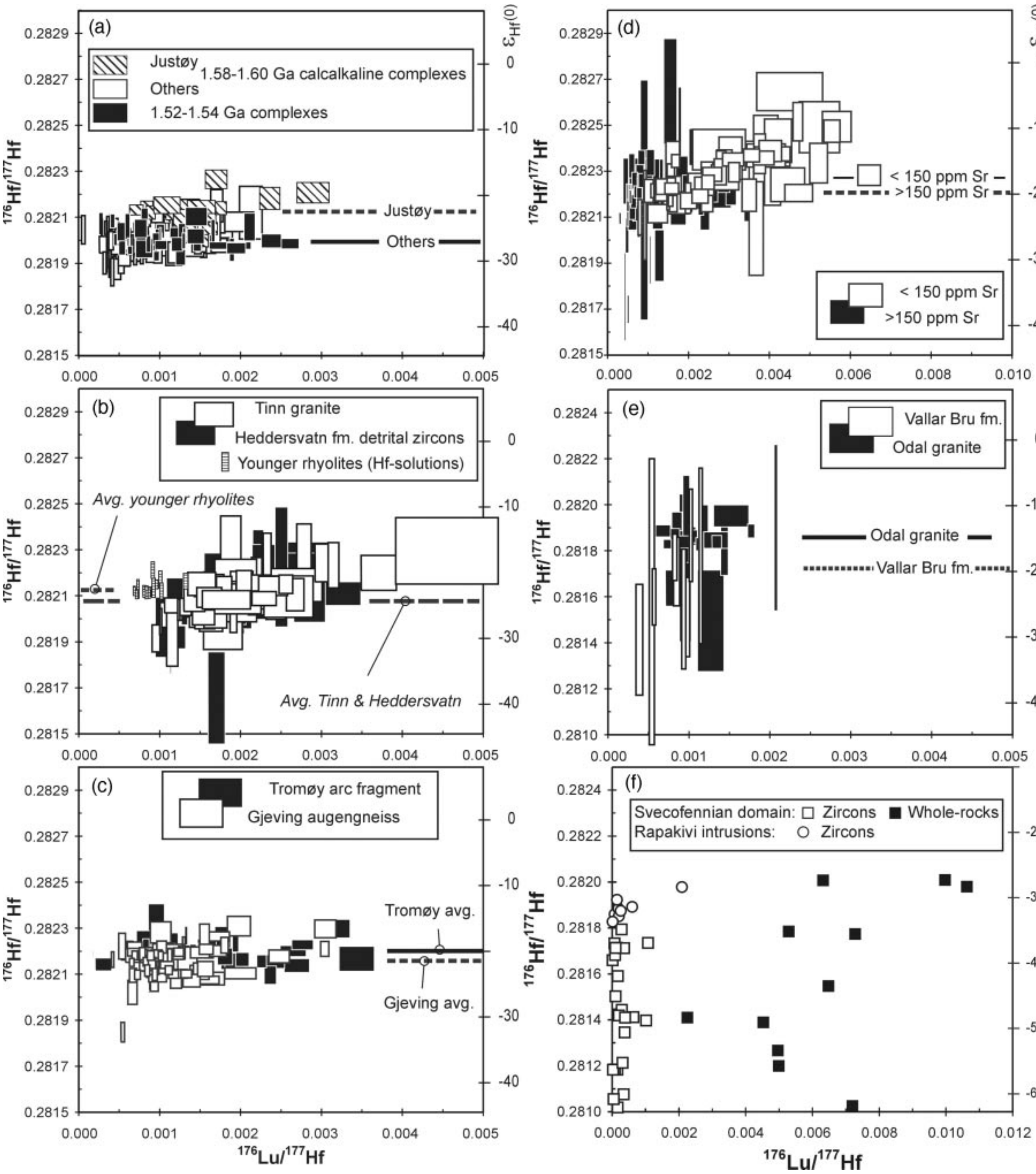

Fig. 2. Lu–Hf correlation diagrams showing the present-day variation in $^{176}Hf/^{177}Hf$ vs $^{176}Lu/^{177}Hf$. (a) Mid-Proterozoic calc-alkaline gneisses. The right-hand scale shows present-day ε_{Hf} values. (b) Younger Telemark meta-rhyolites (solutions), detrital zircons in older Telemark quartzite (Heddersvatn fm) and Tinn granite. For detrital zircons in the younger Telemark quartzites, see (e). (c) Tromøy arc fragment and Sveconorwegian augengneiss. (d) Late Sveconorwegian granites. (e) Detrital zircons from younger Telemark quartzites (Vallar Bru fm) and zircons in the Odal granite (TIB equivalent). (f) Published whole-rock and zircon Lu–Hf data from the eastern and central parts of the Baltic Shield; data from Patchett *et al.* (1981) and Vervoort & Patchett (1996).

$^{176}Hf/^{177}Hf$ from zircons with whole-rock Lu/Hf ratios (Table 4), it is possible to estimate Lu–Hf model ages for the protoliths of most of the rock units analysed in the present study (Fig. 3). For the detrital zircon samples from Telemark metasediments and for non-detrital samples for which no whole-rock trace element data are available, a t_{DMZ} can be calculated, or an approximate t_{DMW} can be estimated from the observed $^{176}Hf/^{177}Hf$ and

Table 4: Lu–Hf and Sm-Nd whole-rock data

Sample	Lu	Hf (ppm)	$^{176}Lu/^{177}Hf$	$^{176}Hf/^{177}Hf$	2σ	Nd	Sm (ppm)	$^{147}Sm/^{144}Nd$	$^{143}Nd/^{144}Nd$	2σ	$\varepsilon_{Nd}(t)$	2σ	$t_{DM}Nd$	2σ
Late Sveconorwegian granites														
072396-3	1·12	18·41	0·008	0·282230	0·000271									
083096-3	0·83	15·2	0·008	0·282213	0·000148									
080296-4	0·43	11·0	0·005	0·282230	0·000093									
082996-2	0·57	13·1	0·006	0·282164	0·000117									
072496-3	0·83	14·8	0·008	0·282211	0·000145									
072496-2	0·52	15·1	0·005	0·282216	0·000154									
072696-2	1·23	7·7	0·022	0·282409	0·000180									
083196-1	1·31	15·0	0·012	0·282266	0·000160									
Mid-Proterozoic granite, Telemark														
071996-2	0·78	7·1	0·015	0·282087	0·000211									
083196-2	0·85	8·5	0·014	0·282106	0·000150									
Sveconorwegian Tromøy arc fragment														
HGG	0·57	3·85	0·021	0·282191	0·000108	16·0	3·0	0·1131	0·511895	0·000010	−1·62	0·20	1·72	0·01
Mid-Proterozoic calc-alkaline gneiss complexes														
TA121/99	0·20	3·99	0·007	0·281998	0·000072	23·4	4·1	0·1059	0·511817	0·000010	1·94	0·20	1·72	0·01
Ø3	0·42	3·97	0·015	0·282010	0·000109	35·2	5·8	0·1003	0·511747	0·000010	2·43	0·20	1·73	0·01
Ø1	0·35	5·31	0·009	0·281986	0·000094	39·0	7·1	0·1254	0·512022	0·000010	2·45	0·20	1·75	0·02
TA116/99	0·37	4·39	0·012	0·281992	0·000124	30·8	6·0	0·1181	0·511983	0·000011	3·18	0·22	1·67	0·02
TA118/99	0·13	3·98	0·005	0·281968	0·000112	21·9	3·5	0·0954	0·511816	0·000011	4·52	0·22	1·57	0·01
10/97NES	0·12	3·56	0·005	0·282053	0·000078	12·0	1·7	0·0895	0·511894	0·000010	7·55	0·20	1·40	0·01
8/97JOM	0·33	5·24	0·009	0·282046	0·000104	22·1	4·5	0·1235	0·511990	0·000011	1·70	0·22	1·76	0·02
5/97JUS	0·16	4·83	0·005	0·282112	0·000075	14·0	3·2	0·1342	0·512324	0·000010	6·66	0·20	1·36	0·02
9/97HOM	0·39	4·03	0·013	0·282141	0·000099	16·0	3·7	0·1445	0·512319	0·000010	4·45	0·20	1·58	0·02

Whole-rock Lu and Hf concentrations on whole rocks, combined with sample-average $^{176}Hf/^{177}Hf$ from Table 3. ε_{Nd} values are calculated at ages given in Table 3.

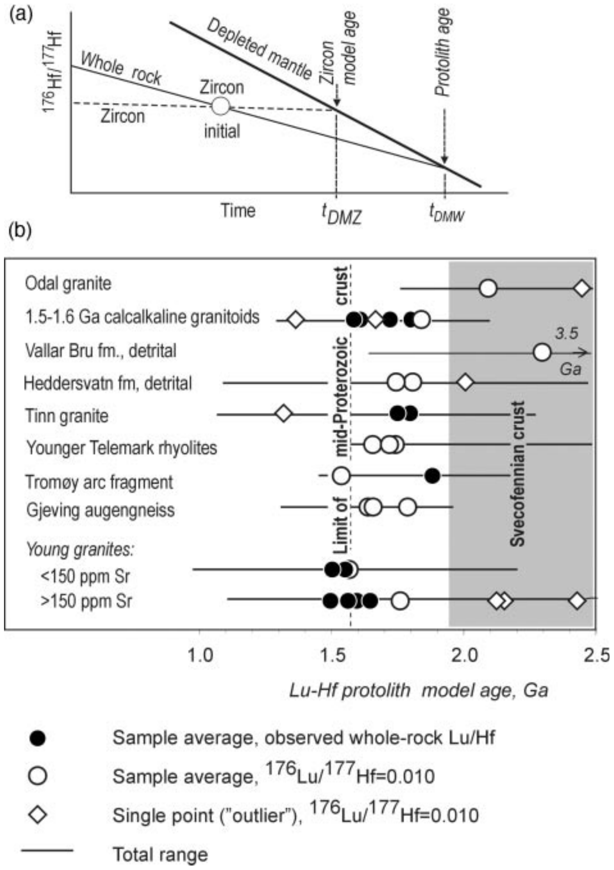

Fig. 3. Crustal residence ages of Hf in the zircons, based on Hf model ages (see text for explanation). (a) The principle of Hf isotope model age calculation, showing the difference between the model age of a zircon (t_{DMZ}) and t_{DMW}, which is a more realistic model age for the protolith of the host-rock. t_{DMW} is calculated forcing a growth-curve with a ^{176}Lu/^{177}Hf ratio corresponding to the host rock through zircon initial ratio. For rocks where no whole-rock concentration data are available, ^{176}Lu/^{177}Hf = 0·010 is used for the calculations. (b) Protolith-ages based on t_{DMW}. ●, model ages calculated using observed whole-rock Lu/Hf ratios (Table 4); ○, model ages estimated from observed initial ^{176}Hf/^{177}Hf of zircons and ^{176}Lu/^{177}Hf = 0·010. The horizontal lines represent the total model age variation within each of the groups, including the ±2SD ranges for each sample.

a representative crustal ^{176}Lu/^{177}Hf ratio. In Table 3 and Fig. 3b, t_{DMW} for such samples was calculated using ^{176}Lu/^{177}Hf = 0·010, which is the average of the whole-rock ^{176}Lu/^{177}Hf ratios reported in Table 4.

The time-corrected ^{176}Hf/^{177}Hf of the mid-Proterozoic tonalitic to granodioritic rocks falls within a range from 0·2819 to 0·2821. There is no systematic trend of initial ^{176}Hf/^{177}Hf with age during this time-interval (Fig. 2a). The two samples from the Justøy tonalite have the highest ^{176}Hf/^{177}Hf of this group. t_{DMW} model ages based on sample averages range from close to the intrusive age for the Justøy complex to 1·8 Ga for intrusions in the Østfold–Akershus Sector.

The mid-Proterozoic rocks from Telemark give somewhat larger total scatter in ^{176}Hf/^{177}Hf (Fig. 2b), but the zircons from the Tinn granite and the detrital zircons from the Heddersvatn formation have similar mean compositions given by ^{176}Hf/^{177}Hf$_m$ of 0·28202 and 0·28204, respectively; the sample averages correspond to t_{DMW} close to 1·7 Ga. Among the Sveconorwegian rocks, the Gjeving augengneiss (^{176}Hf/^{177}Hf$_m$ = 0·28205), the younger rhyolites from Telemark (^{176}Hf/^{177}Hf$_m$ = 0·28212) and the Tromøy complex (^{176}Hf/^{177}Hf$_m$ = 0·28217) have overlapping ranges of time-corrected ^{176}Hf/^{177}Hf (Fig. 2c) and model ages (t_{DMW} = 1·5–1·9 Ga). Zircons from the late Sveconorwegian granites, and the detrital zircons from the Vallar Bru formation (Fig. 2d and e) were analysed in grain mounts originally prepared for secondary ion mass spectrometry (SIMS). The grains in these mounts were small, and polished to a much deeper level than in the other mounts, and as a result many of them gave shorter laser ablation runs, and hence poorer internal precision. This effect is particularly strong for the Vallar Bru zircons (Fig. 2e).

The late Sveconorwegian granites (Fig. 2d), give overall ranges of ^{176}Hf/^{177}Hf$_m$ from 0·28211 to 0·282303 (t_{DMW} = 1·5–1·9 Ga), but a significant group of 'outliers' gives lower ^{176}Hf/^{177}Hf, down to 0·2817, with corresponding t_{DMW} values well above 2·0 Ga. It should be noted that no such low ^{176}Hf/^{177}Hf 'outliers' are observed among granites from central Telemark with low Sr concentrations [these granites, i.e. the 'Group 2 granites' of Andersen *et al.* (2001*a*), should be treated separately from the other late Sveconorwegian granites; see further discussion below]. However, one of the 'low Sr granites' (Otternes) has the highest sample average observed, and contains an outlying single zircon with even higher ^{176}Hf/^{177}Hf, within the range of mantle-derived material (Table 3).

The Odal granite and the detrital zircons in the Vallar Bru quartzite show significantly less radiogenic present-day Hf isotopic compositions (^{176}Hf/^{177}Hf$_m$ $<0{\cdot}21819$, which overlap with the range observed among rocks from the Svecofennian Domain (Fig. 2e and f), and which give t_{DMW} $>2{\cdot}1$ Ga.

New Sm–Nd data on calc-alkaline gneiss complexes are given in Table 4; Sm–Nd data for other rock units analysed for Hf isotopes in this study were published by Andersen (1997), de Haas *et al.* (1999), Knudsen & Andersen (1999) and Andersen *et al.* (2001*a*). Several studies have demonstrated positive correlations between initial Hf and Nd isotopic compositions in juvenile rocks, as well as in rocks with a crustal prehistory (e.g. Vervoort & Patchett, 1996; Vervoort *et al.*, 1999; Vervoort & Blichert-Toft, 1999). With few exceptions, the samples analysed in this study plot close to the correlation lines for both granitic and juvenile systems (Fig. 4). The only sample plotting far outside this range is a garnet-bearing

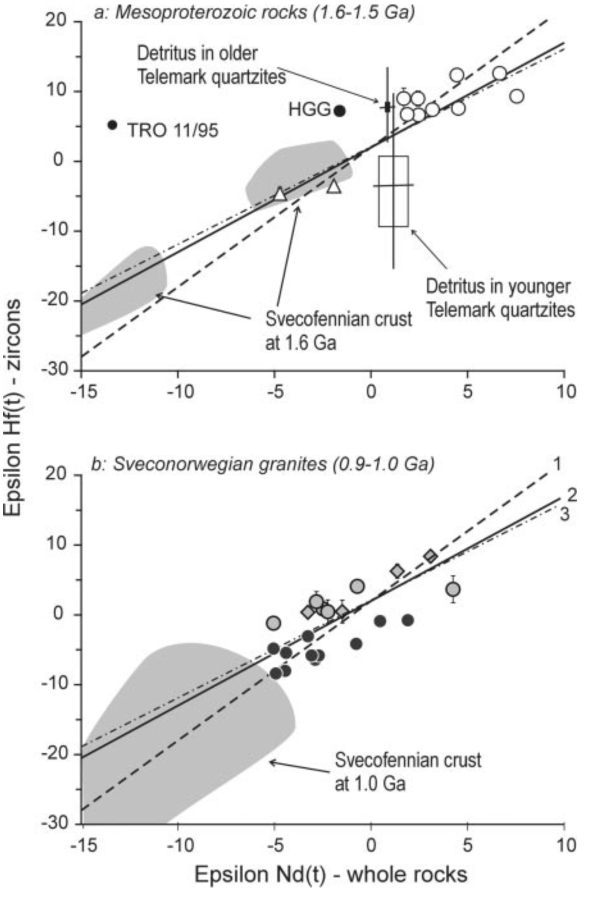

Fig. 4. Correlation of ε_{Hf} of zircons vs ε_{Nd} for whole rocks. Global correlation lines: 1, juvenile crust (Vervoort & Patchett, 1996); 2, the granite correlation line of Vervoort & Patchett (1996); 3, correlation line for juvenile rocks according to Vervoort & Blichert-Toft (1999). The shaded fields represent the range of Svecofennian rocks at 1·6 Ga (a) and 1·0 Ga (b). Sample symbols as in Fig. 1, except for rocks of the Tromøy complex [● in (a)]. (a) Mid-Proterozoic rocks at their age of formation, compared with the range of variation of Svecofennian whole rocks at 1·6 Ga. The Sveconorwegian, calc-alkaline rocks of the Tromøy complex are shown at 1·2 Ga; it should be noted that sample TRO 11/95 is an anatectic trondhjemite, formed by local melting of a mafic gneiss precursor ~70 Myr after its initial crystallization. The anomalous position of this point may reflect an inappropriate combination of Hf data from a 1·2 Ga zircon with Nd data from a garnet-rich 1·1 Ga whole rock. (b) Late Sveconorwegian granites at their age of formation, compared with the range of Svecofennian rocks at 1·0 Ga (shaded field), and the mid-Proterozoic rocks from (a), recalculated to 1·0 Ga (●).

trondhjemite from the Tromøy arc fragment. This vein formed by partial melting of tonalitic or mafic rocks ~70 Myr after their formation in the arc. Knudsen & Andersen (1999) reported a very high $^{147}Sm/^{144}Nd$ ratio of 0·2789, and it is likely that garnet controls the whole-rock Sm–Nd systematics of the vein, whereas the zircons may have been preserved from the protolith; combining a whole-rock ε_{Nd} with ε_{Hf} of zircons may not be justified for this sample. The initial compositions of the late Sveconorwegian granites plot to the high ε_{Nd}–high ε_{Hf} side of both

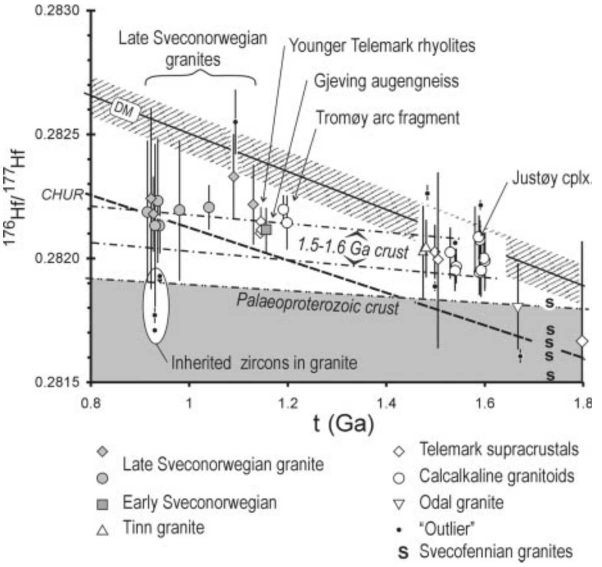

Fig. 5. Hf isotope evolution diagram for the lithological units of south Norway. Each sample is represented by averages of $^{176}Hf/^{177}Hf \pm$ 2SD. Sample symbols are as in Fig. 1, with additional whole-rock and zircon data from Svecofennian granites (Vervoort & Patchett, 1996; Patchett *et al.*, 1981). Growth-curves are shown for CHUR (Blichert-Toft & Albarède, 1997) and depleted mantle (DM, Griffin *et al.*, 2000). The diagonally ruled field surrounding the depleted mantle curve represents a range of compositions of ± 3 ε_{Hf} units, comparable with the range in present-day MORB. Mid-Proterozoic juvenile crust, corresponding to the 1·60–1·52 Ga calc-alkaline gneiss complexes will develop with time within the field delimited by the dash–dot lines. The upper limit of the range of Baltic Shield hafnium is defined by a line through the initial composition of the Odal granite and the highest time-corrected $^{176}Hf/^{177}Hf$ reported from Svecofennian granites (Patchett *et al.*, 1981; Vervoort & Patchett, 1996) with a $^{176}Lu/^{177}Hf = 0{\cdot}005$.

Svecofennian crust and the mid-Proterozoic calc-alkaline gneisses recalculated to 1·0 Ga (Fig. 3b), suggesting that a component more radiogenic than any feasible regional crustal protolith in both Nd and Hf has been involved in their petrogenesis.

DISCUSSION

Hf isotopic characteristics of crustal reservoirs in south Norway

In Fig. 5, time-corrected Hf isotopic compositions of zircons (Table 3) are plotted at their crystallization age, and compared with evolution curves for CHUR (Blichert-Toft & Albarède, 1997) and global depleted mantle (Veervoort & Blichert-Toft, 1999; Griffin *et al.*, 2000). Detrital zircons from the ~1·15 Ga Vallar Bru formation in Telemark have been plotted at an age of 1·80 Ga, corresponding to the U–Pb SIMS age of the old population of detrital zircons identified by de Haas *et al.* (1999), whereas inherited zircons in the late Sveconorwegian granites, which have not been dated, have been plotted at the intrusive age of the host granite.

The zircons and whole rocks from the Svecofennian Domain of the Baltic Shield analysed by Patchett *et al.* (1981) and Vervoort & Patchett (1996) plot at or below a growth curve with $^{176}Lu/^{177}Hf = 0{\cdot}005$ through the the average $^{175}Hf/^{177}Hf$ of the Odal granite at 1·67 Ga. This line is therefore regarded as the upper limit of $^{176}Hf/^{177}Hf$ for continental rocks belonging to the pre-1·7 Ga Baltic Shield. The 1·8 Ga detrital zircons from the younger Telemark supracrustals fall within this field, supporting the conclusion of de Haas *et al.* (1999) that these zircons had a Svecofennian or TIB-related source.

The mid-Proterozoic calc-alkaline gneiss complexes plot within ± 3 ε_{Hf} units of the depleted mantle curve of Griffin *et al.* (2000). Because of the global scarcity of juvenile rocks of mid-Proterozoic age, the Hf-isotopic evolution of the depleted mantle was not previously constrained by data between 1·7 and 0·7 Ga (Vervoort & Blichert-Toft, 1999). The mid-Proterozoic tonalitic to granodioritic metaintrusive gneiss complexes in south Norway have ages in the older part of this interval; the present data thus provide additional constraints for the evolution of the global depleted mantle.

The two samples from the Justøy complex have the most depleted initial Hf isotope signature of this group, with averages plotting slightly above the depleted mantle curve. This may suggest a systematic geographical distribution within the region, with more primitive rocks situated to the present SW, in a more distal setting with respect to the mid-Proterozoic continental margin (Fig. 6).

With time, juvenile crust generated at a destructive plate margin at 1·52–1·60 Ga will evolve towards increasing $^{176}Hf/^{177}Hf$ within the field of '1·5–1·6 Ga crust' in Fig. 5. Crustal protoliths generated in this event are likely to be volumetrically important in SW Sweden, and in the Østfold–Akershus, Kongsberg and Bamble sectors of south Norway. The $\sim$1·5 Ga rocks from Telemark (1·48 Ga Tinn granite and detrital zircons of the Heddersvatn formation) form another tightly clustered group in terms of hafnium isotopic signature. Outlying zircons from the Tinn granite plot above the mantle curve, giving independent support for juvenile, mantle-derived material being involved in its petrogenesis. After their formation, the mid-Proterozoic rocks from Telemark have evolved along growth curves indistinguishable from those of calc-alkaline crust formed in the slightly earlier subduction-related tectonomagmatic event(s) (Fig. 5). This type of crust is distinguished by a negative Sr concentration anomaly, and forms a distinct reservoir in central Telemark, where it was involved in the generation of the late-Sveconorwegian 'low-Sr' granites (Andersen & Knudsen 2000; Andersen *et al.*, 2001*a*).

The initial $^{176}Hf/^{177}Hf$ of zircons from the 1·2 Ga Tromøy arc fragment, the Gjeving augengneiss and the younger Telemark rhyolites all plot close to the upper limit of the 1·5–1·6 Ga crust. Knudsen & Andersen (1999) interpreted Nd, Sr and Pb data from Tromøy as evidence of mixing of juvenile mantle material and pelagic sediments in a subduction zone offshore from the Baltic Shield. The present data are compatible with this interpretation, but do not provide additional constraints on the process. From their Hf isotope signature, the parent magmas of the Gjeving augengneiss and the 1·15 Ga Telemark rhyolites may have been derived from different combinations of depleted mantle-derived material, calc-alkaline crust, older continental rocks and, in the case of the younger Telemark rhyolites, also 1·5 Ga Telemark rhyolites and granites. From Sr and Nd isotope data, Simonsen (1997) suggested that the Gjeving augengneiss formed by mixing of a 1·15 Ga mantle-derived component and a shallow-crustal component similar to the metasedimentary gneisses of the Bamble Sector (Knudsen *et al.*, 1997*a*), which is in agreement with the Hf isotope data.

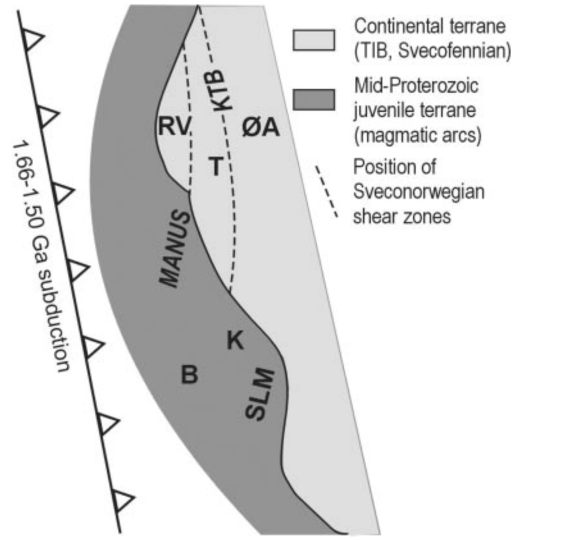

Fig. 6. A mid-Proterozoic tectonic scenario for the margin of the SSD, based on a model by Starmer (1996), modified to account for the presence of continental protoliths in the Telemark and Rogaland–Vest Agder sectors. The positions of some of the present crustal units relative to the mid-Proterozoic continental margin are indicated (abbreviations as in Fig. 1; except SLM, Stora Le–Marstrand belt of SW Sweden). (See further discussion in the text.)

Sveconorwegian granites and crust–mantle interaction

The initial Hf isotopic compositions of the late Sveconorwegian granites plot between the field of Baltic Shield hafnium and the depleted mantle, partly overlapping the $^{176}Hf/^{177}Hf$ ratios of calc-alkaline rocks generated in the mid-Proterozoic event and the range of the older Telemark supracrustals (Fig. 5). From geological evidence, mid-Proterozoic calc-alkaline protoliths are unlikely to have been involved in the petrogenesis of the late Sveconorwegian granites in the Telemark and Rogaland–Vest Agder sectors, as no such rocks have been recorded in these areas (Dons & Jorde, 1978; Falkum, 1982; Padget & Brekke, 1996; Sigmond, 1998; de Haas *et al.*, 1999).

Whole-rock Sr–Nd–Pb isotope data on late Sveconorwegian granites from the entire region define mixing trends between crustal components and a component with a juvenile isotopic signature (Andersen *et al.*, 2001*a*): a Palaeoproterozoic crustal component was involved in the petrogenesis of the granites plotted as shaded circles in Fig. 5, whereas material equivalent to the Rjukan group rhyolite or the 1·48 Ga Tinn granite contributed to the 'low Sr' granites, represented by shaded diamonds. Identification of an endmember with a positive ε_{Nd} does not necessarily indicate that mantle-derived magmas were injected into the crust at the time of deep crustal melting; in fact, such a component may reside in mafic rocks within the deep crust for several hundred million years without totally losing its depleted mantle Nd isotopic signature. There is evidence of mafic magmatism in south Norway both at ~1·5 Ga (Dahlgren *et al.*, 1990*a*; Brewer & Menuge, 1998; Nijland *et al.*, 2000) and in Sveconorwegian time (e.g. Dahlgren *et al.*, 1990*b*; Munz & Morvik, 1991*a*, 1991*b*; de Haas *et al.*, 2000), which suggests that mafic underplating may have taken place during either or both of these periods.

The Hf isotope data are compatible with this petrogenetic model, and provide some further constraints for the timing of mafic underplating. Inherited zircons with Hf isotopic compositions well within the range of pre-1·7 Ga Baltic Shield protoliths at the time of granite emplacement (Fig. 5) suggest the involvement of such old source rocks in the generation of granitic magma. The high average $^{176}Hf/^{177}Hf$ in some of the granites (Otternes, Gunnarstul, Rosskreppfjord), and the overall range towards even more elevated $^{176}Hf/^{177}Hf$ in the Otternes granite, suggest that mantle-derived material may have been introduced significantly later than 1·50 Ga, perhaps as late as 1·2–1·15 Ga, the time of early Sveconorwegian mafic magmatism and the younger period of volcanism in Telemark (Munz & Morvik, 1991*a*, 1991*b*; Laajoki *et al.*, 2000). This does not exclude the additional presence of older, mafic material within the unexposed crust in the region; juvenile material was also involved in the 1·51–1·48 Ga magmatism in Telemark (Andersen *et al.*, 2001*a*, 2001*b*).

The presence of pre-1·7 Ga continental rocks west of the Oslo Rift

Throughout the mid- to late Protoerozoic, evolved continental rocks older than 1·7 Ga have acted as a potential source of unradiogenic Hf with $^{176}Hf/^{177}Hf < 0{\cdot}2820$ (Fig. 5). Such rocks are exposed within the Trans-Scandinavian Igneous Belt and the Svecofennian Domain, where they may have provided a source for far-transported detrital zircons; for example, to the younger clastic sediments in Telemark (de Haas *et al.*, 1999). However, the recognition of material with 1·7–1·9 Ga crustal residence age within the source of late Sveconorwegian granites (Andersen *et al.*, 2001*a*), and the presence of inherited zircons with a Baltic Shield Hf isotopic signature (Fig. 5) suggest that similar rocks are also present in the deep crust of south Norway, where they most probably make up the 'Normal Deep Crust' component identified by Andersen & Knudsen (2000). This regional crustal endmember is characterized by elevated incompatible element concentrations, close to an average 'upper continental crust' level. It shows no depletion in Rb or other large ion lithophile elements (LILE), and has low present-day ε_{Nd} (≤ -15) and elevated $^{87}Sr/^{86}Sr \geq 0{\cdot}74$, indicative of crustal residence since the Palaeoproterozoic.

Towards a model of crustal evolution for the southwestern part of the Baltic Shield

A schematic tectonic scenario for the western margin of the Baltic Shield in the mid-Proterozoic is shown in Fig. 6. The sketch is based on a model by Starmer (1996), modified to account for the results of Andersen & Knudsen (2000), Andersen *et al.* (2001*a*, 2001*c*), Bingen *et al.* (2001) and the present work, which indicate the presence of pre-1·7 Ga crustal protoliths in the Telemark and Rogaland–Vest Agder sectors. There is evidence of calc-alkaline magmatism in the Southwest Scandinavian Domain from ~1·66 to 1·50 Ga, suggesting long-lived subduction off the continental margin (Brewer *et al.*, 1998; Nordgulen, 1999; Andersen *et al.*, 2001*c*). With the exception of the rocks of the Stora Le–Marstrand and Østfold supracrustals and the rocks of the Kongsberg complex, which show a tholeiitic character suggesting an oceanic island-arc environment (Jacobsen, 1975; Brewer *et al.*, 1998; Andersen *et al.*, 2001*c*), calc-alkaline rocks formed throughout this period have a rather uniform major and trace element signature. This signature suggests an immature to moderately mature volcanic arc setting at a continental margin (Brewer *et al.*, 1998; Andersen *et al.*, 2001*c*). The present Hf isotope data are consistent with a major contribution of material derived from a depleted mantle source in these rocks.

When calc-alkaline magmatism ended at ~1·50 Ga, extensional basins were forming in the Telemark Sector, with anorogenic, rhyolite-dominated volcanism (Menuge & Brewer, 1996), possibly in response to a separate, continental rifting event (Sigmond *et al.*, 1997).

Accepting the accumulated evidence that south Norway west of the Oslo Rift is an integral part of the Baltic

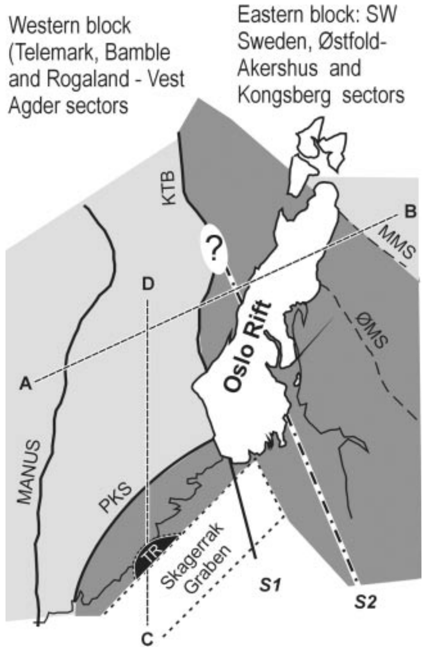

Fig. 7. The present-day crustal architecture of south Norway, with major tectonic boundaries. S1 and S2 are possible locations of Sveconorwegian sinistral strike-slip displacement of the Telemark Sector. Lines AB and CD are profile lines shown in Fig. 8. TR, Tomøy complex. Other abbreviations as in Fig. 1.

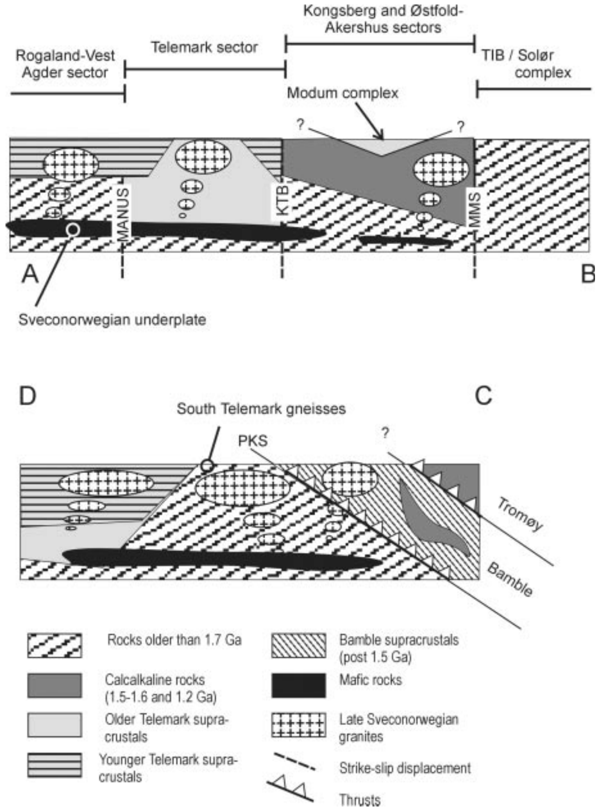

Fig. 8. Schematic NE–SW and north–south cross-sections (not to scale) of the Precambrian crust of south Norway. The positions of the profiles are indicated in Fig. 7. The profiles are based on the distribution of geochemically distinct reservoirs in the continental crust in south Norway derived by Andersen & Knudsen (2000), radiogenic isotope data from late Sveconorwegian granites from Andersen *et al.* (2001*a*), and the data of the present work. (See further discussion in the text.)

Shield (Andersen *et al.*, 2001*a*, 2001*c*; Bingen *et al.*, 2001), the present-day crustal configuration in the region must reflect Sveconorwegian terrane displacement (Fig. 7). The boundary between the mid-Proterozoic calc-alkaline terrane(s) in the Kongsberg and Østfold–Akershus sectors, and the rocks of continental affinity in the Telemark Sector (KTB) is one of the fundamental, sinistral strike-slip boundaries in the region; the MANUS line may be another (Starmer, 1996). In Fig. 7, two alternatives for the position of the KTB are shown: S1 west of the Kongsberg gneiss complex (Andersen *et al.*, 2001*c*; Fig. 1) and S2 further east (Bingen *et al.*, 2001). If future work on the poorly constrained mid-Proterozoic calc-alkaline gneisses of the Kongsberg complex confirms a correlation with the rocks of the Østfold–Akershus Sector, a position west of the Kongsberg complex, as schematically indicated by S1, is the most realistic solution.

Figure 8 shows two schematic and idealized sections (not to scale) across south Norway at the end of the Sveconorwegian orogeny (i.e. before the late Palaeozoic rifting event). The approximate positions of the sections are indicated in Fig. 7. The profiles take into account evidence of Sveconorwegian strike-slip terrane displacement along the western margin of the Baltic Shield (de Haas *et al.*, 1999; Bingen *et al.*, 2001), and geochemical indications that rocks with an evolved chemical character and a crustal history to 1·7–1·9 Ga are present at depth, on both sides of the Oslo Rift and the major Sveconorwegian lineaments in the region (Andersen & Knudsen, 2000; Andersen *et al.*, 2001a; this study). Along the NE–SW section (Fig. 8a), the Mjøsa–Magnor mylonite zone (MMS) separates exposed rocks of the Trans-Scandinavian Igneous Belt (Solør complex) from mid-Proterozoic calc-alkaline rocks, possibly deposited on an older continental margin basement that may consist of TIB-related rocks (Nordgulen, 1999; Andersen & Knudsen, 2000; Andersen *et al.*, 2001*c*). The Østfold–Akershus and Kongsberg sectors may themselves consist of several mid-Proterozoic or Sveconorwegian subterranes (e.g. Bingen *et al.*, 2001), which are not separated here. The pre-1·43 Ga metasedimentary rocks of the Modum complex have a continental signature, and a possible affinity with the older quartzites in Telemark and metasediments in the Bamble Sector (Åhäll *et al.*, 1998; Andersen & Grorud, 1998; Bingen *et al.*, 2001). The northern and central parts of the Telemark Sector are built up of the older

(∼1·50 Ga) and younger (∼1·15 Ga) supracrustal sequences, deposited on an unidentified basement. However, the presence of late Sveconorwegian granites derived from Palaeoproterozoic source rocks within this area points to the presence of 1·7–1·9 Ga basement rocks beneath the supracrustal cover (Andersen *et al.*, 2001*a*). West of the MANUS shear zone, rocks of the younger supracrustal sequence are deposited on a gneissic basement. Again, data from late Sveconorwegian granites suggest the presence of Palaeoproterozoic rocks in the lower crust west of this shear zone (Andersen *et al.*, 2001*a*).

In the north–south section (Fig. 8b), the Bamble Sector is interpreted as a Sveconorwegian nappe, thrust above the gneisses of south Telemark, in agreement with the classical interpretation of the Kristiandsand–Porsgrunn shear zone (PKS, e.g. Smithson, 1963). This also is consistent with recent findings that indicate an early phase of top-towards-NW displacement on this shear zone (Andresen & Bergundhaugen, 2001; Bergundhaugen, 2002). Radiogenic isotope data on granites, and the predominance of 1·8 Ga zircons with low ^{176}Hf/^{177}Hf in the younger Telemark quartzites (de Haas *et al.*, 1999; this study), suggest that pre-1·7 Ga rocks with an evolved, continental signature make up a significant fraction of the south Telemark gneisses, together with reworked equivalents of the older Telemark supracrustals (Ploquin, 1980; de Haas *et al.*, 1999; Andersen *et al.*, 2001*a*). The presence of a component with a long crustal history in the late Sveconorwegian Herefoss granite (Andersen, 1997; this study) cannot be taken as evidence that the supracrustal rocks of the Bamble Sector were deposited on a continental basement, as the granite penetrates the Kristiandsand–Porsgrunn shear zone (Smithson, 1963), and the magma was probably generated within the footwall, consisting of south Telemark gneisses.

The rocks of the Tromøy complex are regarded as being in tectonic contact with the rocks of the mainland Bamble Sector. A thrust-plane separating the Tromøy complex from the rocks of the Bamble Sector *sensu stricto* has not yet been recognized in the field (see Padget & Brekke, 1996), but may tentatively be related to the boundary between metamorphic zones C and D of Field *et al.* (1980). These zones have both been affected by Sveconorwegian granulite-facies metamorphism and local anatexis, and differ mainly in their protolith compositions (Knudsen & Andersen, 1999). Alternatively, the boundary may be under the water separating Tromøy and neighbouring islands from the mainland.

CONCLUSIONS

Hafnium isotope data on zircons separated from samples covering the evolution of the continental crust in south Norway from ∼1·7 to 0·9 Ga demonstrate the importance of the Hf isotopic evidence for the understanding of the evolution of the continental crust, on a regional as well as on a global scale. By using the LAM–ICPMS approach, the necessary number of high-quality analyses can easily be obtained, and spatial resolution can be achieved.

New insights gained from the study of Hf isotope systematics in zircons of Precambrian rocks from south Norway include the following.

Individual igneous rocks contain zircons with a range in ^{176}Hf/^{177}Hf significantly larger than the analytical uncertainties. This probably reflects the 'assembly' of the magmas from several batches of magma derived from different source rocks, including the depleted mantle and different types of older crust. This detailed information is revealed by single-grain *in situ* analysis of zircons, but would be lost in the analysis of whole rocks or zircon composites, as it is in whole-rock studies of Sr, Nd or Pb isotopes.

Rocks belonging to the Trans-Scandinavian Igneous Belt and Svecofennian domains of the Baltic Shield are characterized by Hf protolith ages older than 1·9 Ga. Throughout the mid- and late Proterozoic, such rocks have been present as a source for material with ^{176}Hf/^{177}Hf <0·2820. Clastic material derived from such a source may have been transported from exposed rocks to the east of the area studied, but the presence of such components in the deep crust of the Telemark and Rogaland–Vest Agder sectors is demonstrated.

Juvenile, calc-alkaline crust generated in the mid-Proterozoic is present in the Østfold–Akershus, Kongsberg and Bamble sectors, and is characterized by initial ^{176}Hf/^{177}Hf ratios close to depleted mantle values at the time. Material derived from a depleted mantle source also was involved in the petrogenesis of the Rjukan group volcanic rocks and associated rocks in the Telemark Sector.

Sveconorwegian granitic rocks formed by interaction of mid-Proterozoic and Svecofennian continental components with material derived from a depleted mantle source. The lower crust was rejuvenated by mafic underplating during the Sveconorwegian orogeny.

Rocks with a crustal history to the early Proterozoic and a continental geochemical signature are present at depth in the Telemark and Rogaland–Vest Agder sectors, i.e. west of the juvenile mid-Proterozoic areas of the Kongsberg and Østfold–Akershus sectors. This supports a Cordilleran-type model for the mid-Proterozoic evolution of the margin of the Baltic Shield, followed by southward displacement of terranes along the Baltic margin during the Sveconorwegian orogeny, as suggested by Starmer (1996), de Haas *et al.* (1999) and Bingen *et al.* (2001).

ACKNOWLEDGEMENTS

Thanks are due to the following colleagues who have provided well-characterized samples for this study: Geert-Jan de Haas, Kauko Laajoki, Bjørn Sundvoll, Siri Simonsen and Hans-Fredrik Grorud; special thanks go to Fernando Corfu for providing Hf cuts from TIMS dated zircons. Gunborg Bye-Fjeld and Toril Enger (Mineralogical–Geological Museum, University of Oslo), Tom Bradley and Elena Belousova (GEMOC, Macquarie University) gave invaluable technical assistance to the project. T.A. wishes to thank Professor S. Y. O'Reilly for an invitation to Macquarie University. Thanks are due to Bernard Bingen, Jeff Vervoort and an anonymous referee for constructive reviews. This study was made possible by grants from the Norwegian Research Council (grants 110577/410 and 128157/410) and the Faculty of Mathematics and Natural Sciences, University of Oslo.

REFERENCES

Åhäll, K.-I. & Larson, S.-Å. (2000). Growth-related 1·85–1·55 Ga magmatism in the Baltic Shield; a review addressing the tectonic characteristic of Svecofennian, TIB 1-related and Gothian events. *GFF* **122**, 193–206.

Åhäll, K.-I., Cornell, D. H. & Armstrong, R. (1998). Ion probe zircon dating of metasedimentary units across the Skagerrak: new constraints for early Mesoproterozoic growth of the Baltic Shield. *Precambrian Research* **87**, 117–134.

Åhäll, K.-I., Connelly, J. N. & Brewer, T. S. (2000). Episodic rapakivi magmatism due to distal orogenesis? Correlation of 1·69–1·50 Ga orogenic and inboard, 'anorogenic' events in the Baltic Shield. *Geology* **28**, 823–826.

Andersen, T. (1997). Radiogenic isotope systematics of the Herefoss granite, South Norway: an indicator of Sveconorwegian (Grenvillian) crustal evolution in the Baltic Shield. *Chemical Geology* **135**, 139–158.

Andersen, T. & Grorud, H.-F. (1998). Age and lead isotope systematics of uranium-enriched cobalt mineralization in the Modum complex, South Norway: implications for the Precambrian crustal evolution in the SW part of the Baltic Shield. *Precambrian Research* **91**, 419–432.

Andersen, T. & Knudsen, T.-L. (2000). Crustal contaminants in the Permian Oslo Rift, South Norway: constraints from Precambrian geochemistry. *Lithos* **53**, 247–264.

Andersen, T., Andresen, A. & Sylvester, A. G. (2001*a*). Nature and distribution of deep crustal reservoirs in the southwestern part of the Baltic Shield: evidence from Nd, Sr and Pb isotope data on late Sveconorwegian granites. *Journal of the Geological Society, London* **158**, 253–267.

Andersen, T., Andresen, A. & Sylvester, A. G. (2001*b*). Age and petrogenesis of the Proterozoic Tinn granite, South Norway. *Geonytt* **2001**(1), 26.

Andersen, T., Griffin, W. L., Jackson, S. E. & Knudsen, T.-L. (2001*c*). Timing of mid-Proterozoic calcalkaline magmatism across the Oslo Rift: implications for the evolution of the southwestern margin of the Baltic Shield. *Geonytt* **2001**(1), 25–26.

Andresen, A. & Bergundhaugen, Å. (2001). The Nesland–Nelaug shear zone a high-temperature reverse fault reactivated as an extensional (low temperature) shear zone/fault. *Geonytt* **2001**(1), 27.

Bergundhaugen, Å. (2002). Et studium av den tektonometamorfe utviklingen av grensen mellom Bamble- og Telemarksektoren, ved Neslandsvatn. Cand. Scient. thesis, University of Oslo, 117 pp.

Berthelsen, A. (1980). Towards a palinspastic tectonic analysis of the Baltic Shield. In: Cogne, J. & Slansky, M. (eds) *Geology of Europe, from Precambrian to the post-Hercynian Sedimentary Basins. Mémoires du BRGM* **108**, 5–21.

Berthelsen, A., Olerud, S., Sigmond, E. M. O. & Sundvoll, B. (1996). *Geologisk kart over Norge, berggrunnskart; Oslo; 1:250 000*. Trondheim: Norges Geologiske Undersøkelse.

Bingen, B. & van Breemen, O. (1998). Tectonic regimes and terrane boundaries in the high-grade Sveconorwegian belt of SW Norway inferred from U–Pb zircon geochronology and geochemical signature of augen gneiss suites. *Journal of the Geological Society, London* **155**, 143–154.

Bingen, B., Demaiffe, D., Hertogen, J., Weis, D. & Michot, J. (1993). K-rich calc-alkaline augen gneisses of Grenvillian age in SW Norway: mingling of mantle-derived and crustal components. *Journal of Geology* **101**, 763–778.

Bingen, B., Birkeland, A., Nordgulen, Ø. & Sigmond, E. M. O. (2001). Correlation of supracrustal sequences and origin of terranes in the Sveconorwegian orogen of SW Scandinavia: SIMS data on zircon in clastic metasediments. *Precambrian Research* **108**, 293–318.

Blichert-Toft, J. & Albarède, F. (1997). The Lu–Hf geochemistry of chondrites and the evolution of the mantle–crust system. *Earth and Planetary Science Letters* **148**, 243–258.

Brewer, T. S. & Menuge, J. F. (1998). Metamorphic overprinting of Sm–Nd isotopic systems in volcanic rocks: the Telemark Supergroup, southern Norway. *Chemical Geology* **45**, 1–16.

Brewer, T. S., Daly, J. S. & Åhäll, K.-I. (1998). Contrasting magmatic arcs in the Palaeoproterozoic of the south-western Baltic Shield. *Precambrian Research* **92**, 297–315.

Dahlgren, S. H., Heaman, L. & Krogh, T. E. (1990*a*). Geological evolution and U–Pb geochronology of the Proterozoic central Telemark area, Norway (abstract). *Geonytt* **17**(1), 38.

Dahlgren, S. H., Heaman, L. & Krogh, T. E. (1990*b*). Precise U–Pb zircon and baddeleyite age of the Hesjåbutind gabbro, central Telemark area, Southern Norway (abstract). *Geonytt* **17**(1), 38.

de Haas, G. J. L. M., Andersen, T. & Vestin, J. (1999). Application of detrital zircon geochronology to assembly of a Proterozoic terrain—an example from the Baltic Shield. *Journal of Geology* **107**, 569–586.

de Haas, G. J. L. M., Andersen, T. & Nijland, T. G. (2000). Mid-Proterozoic evolution of the South Norwegian lithosphere. *Geonytt* **2000**(1), 56–57.

Dickin, A. P. (1995). *Radiogenic Isotope Geology*. Cambridge: Cambridge University Press, 490 pp.

Dons, J. A. (1960). Telemark supracrustals and associated rocks. In: Holtedahl, O. (ed.) *Geology of Norway. Norges Geologiske Undersøkelse Bulletin*, **208**, 49–58.

Dons, J. A. & Jorde, K. (1978). *Geologisk kart over Norge, berggrunnskart Skien; 1:250 000*. Trondheim: Norges Geologiske Undersøkelse.

Falkum, T. (1982). *Geologisk kart over Norge, bergrunnskart MANDAL—1: 250 000*. Trondheim: Norges Geologiske Undersøkelse.

Field, D., Drury, S. A. & Cooper, D. C. (1980). Rare-earth and LIL element fractionation in high grade charnockitic gneisses, South Norway. *Lithos* **13**, 281–289.

Gaàl, G. & Gorbatschev, R. (1987). An outline of the Precambrian evolution of the Baltic Shield. *Precambrian Research* **35**, 15–52.

Gorbatschev, R. & Bogdanova, S. (1993). Frontiers in the Baltic Shield. *Precambrian Research* **64**, 3–21.

Graversen, O. (1984). Geology and structural evolution of the Precambrian rocks of the Oslofjord–Øyeren area, southeast Norway. *Norges Geologiske Undersøkelse* **398**, 1–50.

Griffin, W. L., Pearson, N. J., Belousova, E., Jackson, S. E., van Achterbergh, E., O'Reilly, S. Y. & Shee, S. R. (2000). The Hf isotope composition of cratonic mantle: LAM–MC-ICPMS analysis of zircon megacrysts in kimberlites. *Geochimica et Cosmochimica Acta* **64**, 133–147.

Griffin, W. L., Wang, X., Jackson, S. E., Pearson, N. J., O'Reilly, S. Y., Xu, X. & Zhou, X. (2002). Zircon chemistry and magma genesis, SE China: *in-situ* analysis of Hf isotopes, Pingtan and Tonglu igneous complexes. *Lithos* **61**, 237–269.

Hageskov, B. (1980). The Sveconorwegian structures in the Norwegian part of the Kongsberg–Bamble–Østfold segments. *Geologiska Föreningen i Stockholms Förhandlingar* **102**, 150–155.

Hjelle, A. (1963). Noen observasjoner fra grunnfjellsområdet mellom Randsfjorden og svenskegrensen. *Norges Geologiske Undersøkelse* **223**, 118–126.

Jacobsen, S. B. (1975). Geochronological, geochemical and petrological investigations of Precambrian rocks in the Kongsberg area. Cand. Real. Thesis, University of Oslo.

Jacobsen, S. B. & Heier, K. S. (1978). Rb–Sr isotope systematics in metamorphic rocks, Kongsberg Sector, south Norway. *Lithos* **11**, 257–276.

Killeen, P. G. & Heier, K. S. (1975). Radioelement distribution and heat production in Precambrian granitic rocks, southern Norway. *Det Norske Videnskaps-Akademi, Matematisk-Naturvitenskapelig Klasse, Skrifter, Ny serie* **35**.

Kleppe, A. V. (1980). Geologiske undersøkelser fra sentrale deler av Telemark med hovedvekt på geokronologi, og kontaktrelasjonen mellom granittisk gneiss og suprakrustalene. Cand. Real. Thesis, University of Oslo, 157 pp.

Knudsen, T.-L. (1996). Petrology and geothermobarometry of granulite-facies metapelites from the Hisøy–Torungen area, South Norway: new data on the Sveconorwegian *p–T–t* path of the Bamble sector. *Journal of Metamorphic Geology* **14**, 267–287.

Knudsen, T.-L. (1997). From protocrust to lower crust: the geochemical evolution of metasediments and associated rocks from the Bamble Sector, southern Norway. Dr. Scient. Thesis, University of Oslo.

Knudsen, T.-L. & Andersen, T. (1999). Petrology and geochemistry of the Tromøy gneiss complex, south Norway, an alleged example of Proterozoic depleted lower continental crust *Journal of Petrology* **40**, 909–933.

Knudsen, T.-L., Andersen, T., Maijer, C. & Verschure, R. H. (1997*a*). Trace element characteristics and selective elemental depletion during medium- to high-grade metamorphism of Proterozoic rocks from the Bamble Sector, southern Norway. *Chemical Geology* **143**, 145–169.

Knudsen, T.-L., Andersen, T., Whitehouse, M. J. & Vestin, J. (1997*b*). Detrital zircon ages from southern Norway—implications for the Proterozoic evolution of the southwestern part of the Baltic Shield. *Contributions to Mineralogy and Petrology* **130**, 47–58.

Kullerud, L. & Dahlgren, S. H. (1993). Sm–Nd geochronology of Sveconorwegian granulite-facies mineral assemblages in the Bamble Shear Belt, South Norway. *Precambrian Research* **64**, 389–402.

Kullerud, L. & Machado, N. (1991). End of a controversy: U–Pb geochronological evidence for significant Grenvillian activity in the Bamble area, Norway. *Terra Abstracts* **3**, 504.

Laajoki, K., Corfu, F. & Andersen, T. (2000). U–Pb zircon dating of the Mesoproterozoic Brunkeberg formation and its bearing on the stratigraphy of Telemark Supracrustals, South Norway. *Journal of Conference Abstracts* **5**(2), 611.

Lindström, M., Lundqvist, J. & Lundqvist, T. (2000). *Sveriges geologi från urtid till nutid.* Lund: Studentlitteratur, 491 pp.

Menuge, J. F. & Brewer, T. S. (1996). Mesoproterozoic anorogenic magmatism in southern Norway. In: Brewer, T. S. (ed.) *Precambrian Crustal Evolution in the North Atlantic Region. Geological Society, London, Special Publications* **112**, 275–295.

Michot, P. (1960). La géologie de la catazone: le problème des anorthosites, la palingenèse basique et al tectonique catazonale dans le Rogaland méridionale. *Norges Geologiske Undersøkelse* **212g**, 1–54.

Munz, I. A. & Morvik, R. (1991*a*). Metagabbros in the Modum complex, southern Norway: an important heat source for Sveconorwegian metamorphism. *Precambrian Research* **52**, 97–113.

Munz, I. A. & Morvik, R. (1991*b*). Metagabbros in the Modum complex, southern Norway: an important heat source for Sveconorwegian metamorphism. Corrigendum. *Precambrian Research* **53**, 305.

Nijland, T. G. (1993). The Bamble amphibolite to granulite facies transition zone, Norway. Ph.D. Thesis, University of Utrecht, Utrecht, 166 pp.

Nijland, T. G., de Haas, G. J. L. M. & Andersen, T. (2000). Rifting-related (sub)alkaline magmatism in the Bamble sector (Norway) during the 'Gothian'–Sveconorwegian interlude. *GFF* **122**, 297–305.

Nordgulen, Ø. (1999). *Geologisk kart over Norge, Berggrunnskart HAMAR, M 1:250 000.* Trondheim: Norges Geologiske Undersøkelse.

Nordgulen, Ø., Tucker, R. D., Sundvoll, B., Solli, A., Nissen, A. L., Zwaan, K. B., Birkeland, A. & Sigmond, E. M. O. (1997). Paleo- to Mesoproterozoic intrusive rocks in the area between Numedal and Mjøsa, SE Norway. In: Nordgulen, Ø., Padget, P., Robinson, P. & McEnroe, S. (eds) *COPENA Conference at NGU, 18–22 August 1997. Abstracts and Proceedings. Norges Geologiske Undersøkelse Report* **97.131**.

Padget, P. & Brekke, H. (1996). *Geologisk kart over Norge, berggrunnskart Arendal, 1:250 000.* Trondheim: Norges Geologiske Undersøkelse.

Patchett, P. J., Kouvo, O., Hedge, C. E. & Tatsumoto, M. (1981). Evolution of continental crust and mantle heterogeneity: evidence from Hf isotopes. *Contributions to Mineralogy and Petrology* **78**, 279–297.

Ploquin, A. (1972). Le granite acide d'Åmli, Norvège méridonale: transformation des laves acides du Tuddal (Formation inférieure des Séries de roches supracrustales du Telemark). *Sciences de la Terre* **17**, 81–95.

Ploquin, A. (1980). Étude géochimique et pétrographique du complex de gneiss, migmatites et granits du Telemark–Aust Agder (Precambrien de Norvège du Sud). Sa place dans l'ensemble épisonal à catazonal profond du Haut Telemark au Bamble. *Sciences de la Terre Mémoire* **38**, 1–389.

Schärer, U., Wilmart, E. & Duschesne, J.-C. (1996). The short duration and anorogenic character of anorthosite magmatism. *Earth and Planetary Science Letters* **139**, 335–350.

Schiellerup, H., Lambert, D. D., Prestvik, T., Robins, B., McBride, J. S. & Larsen, R. B. (2000). Re–Os isotopic evidence for a lower crustal origin of massive-type anorthosites *Nature* **405**, 781–784.

Sigmond, E. M. O. (1997). *The Precambrian Geology of Central Southern Norway. Norges Geologiske Undersøkelse Report* **97.131**.

Sigmond, E. M. O. (1998). *Geologisk kart over Norge. Berggrunnsgeologisk kart, ODDA M 1:250 000.* Trondheim: Norges Geologiske Undersøkelse.

Sigmond, E. M. O., Gjelle, S. & Solli, A. (1997). The Rjukan Proterozoic rift basin, its basement and cover, volcanic, and sedimentary infill, and associated intrusions *Norges Geologiske Undersøkelse Bulletin* **433**, 6–7.

Simonsen, S. L. (1997). Radiogenic isotope systematics of charnockite and retrograded augen gneiss in the Gjeving Complex, South Norway. Cand. Scient. Thesis, University of Oslo, 60 pp.

Smithson, S. B. (1963). Granite studies, 2, the Precambrian Flå granite, a geological and geophysical investigation—gravimetry. *Norges Geologiske Undersøkelse* **219**, 112–122.

Starmer, I. C. (1985). The evolution of the south Norwegian Proterozoic as revealed by the major and mega tectonics of the Kongsberg and Bamble Sectors. In: Tobi, A. C. & Touret, J. L. R. (eds) *The Deep*

Proterozoic Crust in the North Atlantic Provinces. NATO Advanced Study Institute Series, Series C **158**, 259–290.

Starmer, I. C. (1996). Accretion, rifting, rotation and collision in the North Atlantic supercontinent, 1700–950 Ma. In: Brewer, T. S. (ed.) *Precambrian Crustal Evolution in the North Atlantic Region. Geological Society, London, Special Publications* **112**, 219–248.

Sylvester, A. G. (1998). Magma mixing, structure, and re-evaluation of the emplacement mechanisms of Vrådal pluton, central Telemark, southern Norway. *Norsk Geologisk Tidsskrift* **78**, 259–276.

Torske, T. (1985). Terrain displacement and Sveconorwegian rotation of the Baltic Shield: a working hypothesis. In: Tobi, A. C. & Touret, J. L. R. (eds) *The Deep Proterozoic Crust in the North Atlantic Provinces. NATO Advanced Study Institute Series, Series C* **158**, 333–343.

Vervoort, J. D. & Blichert-Toft, J. (1999). Evolution of the depleted mantle: Hf isotope evidence from juvenile rocks through time. *Geochimica et Cosmochimica Acta* **63**, 533–556.

Vervoort, J. D. & Patchett, P. J. (1996). Behaviour of hafnium and neodymium isotopes in the crust: controls from Precambrian crustally derived granites. *Geochimica et Cosmochimica Acta* **60**, 3717–3733.

Vervoort, J. D., Patchett, P. J., Blichert-Toft, J. & Albarède, F. (1999). Relationships between Lu–Hf and Sm–Nd systems in the global sedimentary system. *Earth and Planetary Science Letters* **168**, 79–99.

Wiedenbeck, M., Alle, P., Corfu, F., Griffin, W. L., Meier, M., Oberli, F., Von Quadt, A., Roddick, J. C. & Spiegel, W. (1995). Three natural zircon standards for U–Th–Pb, Lu–Hf, trace element and REE analyses. *Geostandards Newsletter* **19**(1), 1–23.

APPENDIX: SAMPLES FOR Hf ISOTOPE ANALYSIS

Sample	Locality	UTM coordinates E	UTM coordinates N	Petrography	Age (Ga)	Method	Sources of data
Late Sveconorwegian granites (Sr >150 ppm)							
107/92	Herefoss	4594	64804	Granite ('postorogenic')	0·93	Pb–Pb minerals	Andersen (1997)
072396-3	Tovdal	4544	65170	Granite ('postorogenic')	0·94	SIMS U–Pb, zircon	Andersen *et al.* (2001*a*, in preparation)
083096-3	Byklom	4083	65833	Granite ('postorogenic')	0·98	SIMS U–Pb, zircon	Andersen *et al.* (2001*a*, in preparation)
080296-4	Rosskreppfjord	3939	65493	Granite ('postorogenic')	1·04	SIMS U–Pb, zircon	Andersen *et al.* (2001*a*, in preparation)
082996-2	Høvring	4396	65014	Granite ('postorogenic')	0·94	SIMS U–Pb, zircon	Andersen *et al.* (2001*a*, in preparation)
072496-3	Sæbyggjenut	4254	65926	Granite ('postorogenic')	0·94	SIMS U–Pb, zircon	Andersen *et al.* (2001*a*, in preparation)
Late Sveconorwegian granites (Sr <150 ppm)							
072196-3	Bandak	4658	65849	Granite ('postorogenic')	0·93	SIMS U–Pb, zircon	Andersen *et al.* (2001*a*, in preparation)
072496-2	Bessefjell	4412	65973	Granite ('postorogenic')	0·93	SIMS U–Pb, zircon	Andersen *et al.* (2001*a*, in preparation)
072696-2	Otternes	5149	65794	Granite ('postorogenic')	1·09	SIMS U–Pb, zircon	Andersen *et al.* (2001*a*, in preparation)
083196-1	Gunnarstul	4873	66067	Granite ('postorogenic')	1·13	SIMS U–Pb, zircon	Andersen *et al.* (2001*a*, in preparation)
Mid-Proterozoic granite, Telemark							
083196-2	Tinn	4862	66509	Deformed granite	1·48	SIMS U–Pb, zircon	Andersen *et al.* (2001*a*, 2001*b*)
071996-2	Tinn	4908	66523	Deformed granite	1·48	SIMS U–Pb, zircon	Andersen *et al.* (2001*a*, 2001*b*)
Sveconorwegian granitic augengneiss ('Gjerstad suite')							
G2/94	Gjeving	5036	64986	Granitic augengneiss	1·15	TIMS U–Pb, zircon	Kullerud & Machado (1991), Simonsen (1997)
G16/94	Gjeving	5037	64987	Granitic augengneiss	1·15	TIMS U–Pb, zircon	Kullerud & Machado (1991), Simonsen (1997)
G9/94	Gjeving	5036	64987	Granitic augengneiss	1·15	TIMS U–Pb, zircon	Kullerud & Machado (1991), Simonsen (1997)
TIB granite							
SA4A	Odal	6308	67258	Two-feldspar granite	1·67	TIMS U–Pb, zircon	Nordgulen (1999), B. Sundvoll (personal communication, 2000)

Sample	Locality	UTM coordinates E	UTM coordinates N	Petrography	Age (Ga)	Method	Sources of data
Sveconorwegian Tromøy arc fragment							
TRO11/95	Tromøy	4898	64808	Trondhjemite	1·20	SIMS U–Pb, zircon	Knudsen & Andersen (1999)
HGG	Hisøy	4843	64764	Tonalitic gneiss	1·20	LAM–ICPMS U–Pb, zircon	Andersen *et al.* (2001*c*)
Mid-Proterozoic calc-alkaline gneiss complexes							
HFG	Snarum	5452	66584	Granodiorite	1·54	LAM–ICPMS U–Pb, zircon	Nordgulen (1999), H. F. Grorud (personal communication, 2000)
TA121/99	Sørmarka	6034	66273	Granodiorite	1·54	LAM–ICPMS U–Pb, zircon	Andersen *et al.* (2001*c*)
Ø3	Feiring	6105	66423	Quartz diorite	1·60	LAM–ICPMS U–Pb, zircon	Andersen *et al.* (2001*c*)
Ø1	Tistedal	6440	65578	Granodiorite	1·58	LAM–ICPMS U–Pb, zircon	Andersen *et al.* (2001*c*)
TA116/99	Midtskog	6278	66391	Tonalite	1·58	LAM–ICPMS U–Pb, zircon	Andersen *et al.* (2001*c*)
TA118/99	Bjørkelangen	6417	66343	Granodiorite	1·58	LAM–ICPMS U–Pb, zircon	Andersen *et al.* (2001*c*)
10/97NES	Gjerstadvatn	5029	65247	Tonalite	1·60	LAM–ICPMS U–Pb, zircon	Andersen *et al.* (2001*c*)
5/97JUS	Justøy–Justøy	4624	64517	Granodiorite	1·59	LAM–ICPMS U–Pb, zircon	Andersen *et al.* (2001*c*)
9/97HOM	Justøy–Homborsund	4707	64595	Tonalite	1·59	LAM–ICPMS U–Pb, zircon	Andersen *et al.* (2001*c*)
8/97JOM	Jomås	4761	64968	Tonalite	1·53	LAM–ICPMS U–Pb, zircon	Andersen *et al.* (2001*c*)
Detrital zircons, Telemark supracrustals							
KL291	Heddersvatn fm	4550	66004	Quartzite (detrital zircons)	1·50	SIMS U–Pb, zircon	Andersen & Laajoki (in preparation)
KL78·2	Heddersvatn fm	4785	66053	Quartzite (detrital zircons)	1·50	SIMS U–Pb, zircon	Andersen & Laajoki (in preparation)
GA 526	Vallar Bru fm	4742	65898	Quartzitic conglomerate (detrital zircons)	1·80	SIMS U–Pb, zircon	de Haas *et al.* (1999), Laajoki *et al.* (2000)
Young Telemark rhyolites							
903 KL-N	Brunkeberg fm	4707	65911	Meta-rhyolite	1·15	TIMS U–Pb, zircon	Laajoki *et al.* (2000)
TA 99/2 O	Heddal gr	4926	66146	Meta-rhyolite	1·15	TIMS U–Pb, zircon	Laajoki *et al.* (2000)
830 O13	Ofte fm	4606	65911	Meta-rhyolite	1·15	TIMS U–Pb, zircon	Laajoki *et al.* (2000)